Award Number: W81XWH-12-1-0436

TITLE: TrkB Activators for the Treatment of Traumatic Vision Loss

PRINCIPAL INVESTIGATOR: Michael P. Luvone

CONTRACTING ORGANIZATION: Emory University
Atlanta, GA 30322

REPORT DATE: June 2017

TYPE OF REPORT: Final

PREPARED FOR: U.S. Army Medical Research and Materiel Command
Fort Detrick, Maryland 21702-5012

REPORT DOCUMENTATION PAGE

Form Approved
OMB No. 0704-0188

1. REPORT DATE	2. REPORT TYPE	3. DATES COVERED
June 2017	Final	30Sept2012 - 29Mar2017

4. TITLE AND SUBTITLE
TrkB Activators for the Treatment of Traumatic Vision Loss

5a. CONTRACT NUMBER

5b. GRANT NUMBER
W81XWH-12-1-0436

5c. PROGRAM ELEMENT NUMBER

6. AUTHOR(S)
Michael P. Luvone

E-Mail: miuvone@emory.edu

5d. PROJECT NUMBER

5e. TASK NUMBER

5f. WORK UNIT NUMBER

7. PERFORMING ORGANIZATION NAME(S) AND ADDRESS(ES)
Emory University
1365B Clifton Rd NE
Atlanta, GA 30322

8. PERFORMING ORGANIZATION REPORT NUMBER

9. SPONSORING / MONITORING AGENCY NAME(S) AND ADDRESS(ES)
U.S. Army Medical Research and Materiel Command
Fort Detrick, Maryland 21702-5012

10. SPONSOR/MONITOR'S ACRONYM(S)

11. SPONSOR/MONITOR'S REPORT NUMBER(S)

12. DISTRIBUTION / AVAILABILITY STATEMENT
Approved for Public Release; Distribution Unlimited

13. SUPPLEMENTARY NOTES

14. ABSTRACT
Pressure waves due to explosions can damage the neurons of the eye and visual centers in the brain, leading to functional loss of vision. There are currently few treatments for such injuries that can be deployed rapidly in the field to mitigate such damage. Our research team is developing small molecule activators of TrkB, the cognate receptor for brain-derived neurotrophic factor (BDNF), which can be administered systemically and cross the blood brain/retina barrier (BBB). In the third year of the grant, we tested the effects of the TrkB receptor activator, HIOC, in a blast overpressure model of ocular trauma. HIOC produced a significant preservation of visual function, which in some experiments was nearly complete. We also found that HIOC partially prevented optic nerve degeneration, astrocytosis, and thinning of the retinal ganglion cell / nerve fibers following ocular blast injury. We also found that HIOC prevented the loss of visual function caused by blast directed at the head.

15. SUBJECT TERMS
trauma, neuroprotection, retina, optic nerve, TrkB, BDNF, brain, TBI

16. SECURITY CLASSIFICATION OF:			17. LIMITATION OF ABSTRACT	18. NUMBER OF PAGES	19a. NAME OF RESPONSIBLE PERSON
a. REPORT	b. ABSTRACT	c. THIS PAGE			USAMRMC
U	U	U	UU	69	19b. TELEPHONE NUMBER *(include area code)*

Table of Contents

Page

1. Introduction…… 3

2. Keywords…… 3

3. Overall Project Summary……..... 3

4. Key Research Accomplishments……..... 20

5. Conclusion……..... 21

6. Publications, Abstracts, and Presentations……... 21

7. Inventions, Patents and Licenses……... 22

8. Reportable Outcomes..……..... 22

9. Other Achievements……..... 22

10. References……..... 22

11. Personnel……..... 23

12. Appendices…….24

1. INTRODUCTION

Pressure waves due to explosions can damage the neurons of the eye and visual centers in the brain, leading to functional loss of vision. There are currently few treatments for such injuries that can be deployed rapidly in the field to mitigate such damage. Our research team is developing small molecule activators of TrkB, the cognate receptor for brain-derived neurotrophic factor (BDNF). BDNF has been shown to have neuroprotective effects in a number of degeneration models, including optic nerve crush and bright light-induced retinal degeneration (Gauthier et al., 2005; Weber et al., 2010). However, BDNF must be injected intraocularly or into the brain to be effective, as it does not cross the blood brain/retina barrier (BBB), making it impractical to deploy in the field. In contrast, the compounds we are developing can be administered systemically and readily cross the BBB (Jang et al., 2010a,b,c). Following peripheral injection, the drugs activate TrkB receptors in the retina and the brain, and appear to show no systemic toxicity. In preliminary studies, we have shown that they protect against light-induced retinal degeneration (Shen et al., 2012). The goal of this project is to develop effective treatments for traumatic blast-related retinal and visual system damage that can be delivered on the battlefield. We hypothesize that small molecule activators of TrkB will be useful for this purpose. We proposed 3 specific aims to test this hypothesis, investigating the utility of TrkB activators to prevent retinal ganglion cell death following optic nerve crush, protect retinal cells from blast-induced injury to the eye, and protect central visual pathways from traumatic blast-induced injury.

2. KEYWORDS: trauma, neuroprotection, retina, optic nerve, TrkB, BDNF, brain, TBI

3. OVERALL PROJECT SUMMARY

The statement of work for year 4 was to complete the test of TrkB activators for treatment of blast-induced degeneration in visual pathways in the brain. These studies are still underway, but will be completed before the end of the no cost extension. We added new experiments to aim 2 to further characterize the protective effect of HIOC against ocular blast, as well as conducting experiments on effects of HIOC on visual function following TBI. Our studies demonstrate that HIOC, our lead TrkB activator, significantly reduces loss of visual function following blast injury to the eye and to the brain.

In year 1, experiments were initiated to establish assays for measuring retinal ganglion cell (RGC) loss after optic nerve crush. Three approaches were taken. One was to count Brn3a immunoreactive cells in retinal whole mounts. Brn3a is a specific marker for retinal ganglion cells (Nadal-Nicolas et al., 2009); it is expressed by approximately 90% of ganglion cells. The other approach was to count fluorescent RGCs of Thy1-CFP mice, which express CFP (cyan fluorescent protein) in retinal ganglion cells (Feng et al., 2000), or to measure fluorescence in retinal extracts of these mice. We initiated studies on effects of TrkB agonists on RGC loss following optic nerve crush, but found that systemic injection did not have a consistent neuroprotective effect.

In year 2, we investigated the effects of HIOC, delivered by various routes (i.p. or osmotic minipump), in combination with a variety anti-inflammatory and microglial-modulating drugs on optic nerve crush-induced retinal ganglion cell degeneration. None were effective. We concluded that such severe injury to the optic nerve might be beyond pharmacological intervention, at least with our tools. We built and calibrated the blast cannon, and initiated experiments to test the efficacy of TrkB activators on loss of visual function following blast-induced damage to the eye. In preliminary studies we showed potential efficacy of HIOC in preventing loss of visual function caused by blast-induced damage to the eye.

In year 3, we demonstrated that HIOC was effective in reducing vision loss and optic nerve axon degeneration following blast injury to the eye, that this effect was blocked by a TrkB antagonist, that the drug could be administered up to 3 hours after exposure to blast and still have a beneficial therapeutic effect. We also initiated studies to examine the effects of blast injury to the head on visual function and present the preliminary results of HIOC administered after blast on visual function. The results are detailed below.

During year 4 and the 6 month no cost extension, we conducted a dose-response study for the effect of HIOC on preservation of visual function following ocular blast. We demonstrated that the effect of HIOC on visual function preservation is due to its action on TrkB receptors. We found that HIOC reduced ocular blast-induced astrocytosis and thinning of the ganglion cell / nerve fiber layer. HIOC also reduced ocular blast-induced microglial activation. We showed that HIOC is more efficacious than two other BDNF receptor ligands, and examined the effect of repeated mild ocular blast on visual function. We also examined the effect of different blast pressures on head blast (TBI)-induced loss of visual function, and showed that head blast causes cerebral microglial activation. We conducted a dose-response analysis of the effect HIOC on TBI-induced loss of visual function, and found that 80 mg/kg i.p. completely prevented the decline in visual acuity and contrast sensitivity.

3A. Specific Aim 1. To examine the ability of TrkB activators to prevent retinal ganglion cell (RGC) death and loss of visual function following optic nerve crush.

The statement of work was to use the optic nerve crush model to test the effects of small molecule TrkB activators on RGC survival following optic nerve crush. In order to do this, we needed to establish the optic nerve injury model in our lab and develop assays for retinal ganglion cell death. Only key experiments are presented here; additional detail can be found in the annual reports.

Experiments were initiated to establish assays for measuring RGC loss after optic nerve crush. Two approaches were taken. One was to count Brn3a immunoreactive cells in retinal whole mounts. Brn3a is a specific marker for retinal ganglion cells (Nadal-Nicolas et al., 2009); it is expressed by approximately 90% of ganglion cells. The other approach was to measure fluorescence of retinal extracts of Thy1-CFP mice, which express cyan fluorescent protein in retinal ganglion cells (Feng et al., 2000).

Immunofluorescent Staining of Retinal Ganglion Cells - We have optimized an immunostaining protocol that allows for detection of retinal ganglion cells in retinal flatmounts. The majority of RGCs can be stained with antibodies against the RGC marker Brn-3a and visualized by fluorescent microscopy. Brn-3a also has the advantage of being a nuclear marker, so cell bodies can be easily identified and counted. This has been useful for examining the RGC damage and death time course after optic nerve crush (Figure 1).

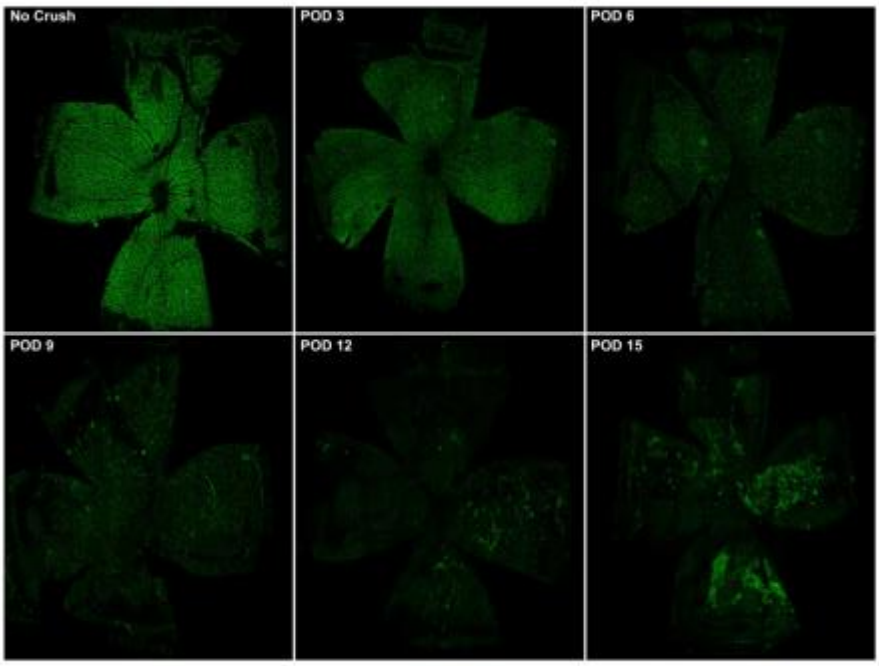

Figure 1. Time course of RGC signal following optic nerve crush. Confocal images of retinal flatmounts were taken every three days over a 15 day period to show the progression of RGC loss after optic nerve crush. POD = post-operation day.

As can be seen in Figure 1, maximal retinal ganglion cell loss occurs approximately 6 days after optic nerve crush.

Measurement of Fluorescence of Thy1-CFP ganglion cells. Our initial studies assessing retinal ganglion cell death following optic nerve crush involved counting Brn3a positive ganglion cells, labeled immunocytochemically, in retinal whole mounts. The procedure is extremely time consuming, taking approximately one week to complete the analysis following euthanizing the mice. The new procedure involved the use of transgenic Thy1-CFP mice, whose retinal ganglion cells express cyan fluorescent protein, and measuring fluorescence of retinal supernatant fractions using a microplate reader. Briefly, optic nerve crush surgery was performed on the right eye, with the left eye serving as the uncrushed control. The mice were euthanized 6 days thereafter. Retinas were immediately dissected and frozen. Retinal homogenates were prepared in RIPA buffer with a protease inhibitor cocktail. Retinal homogenates were centrifuged for 10 minutes. Each supernatant fraction was plated in triplicate on a black 96-well plate and the relative levels of fluorescence

were detected by a BioTek H1 plate reader. In a separate cohort of mice, Brn3a positive retinal ganglion cells were counted. As seen in Figure 1, the percentage decrease in Brn3a positive cells following optic nerve crush was nearly identical to the decrease in CFP fluorescence measured in the plate reader. A number of control experiments were performed to further validate the assay (not shown). The new assay takes only hours, as opposed to days for counting the Brn3a positive cells. The rate-limiting factor is breeding and genotyping the Thy1-CFP mice. This work was presented at the International Society for Eye Research (ISER) Molecular Mechanisms of Glaucoma Symposium.

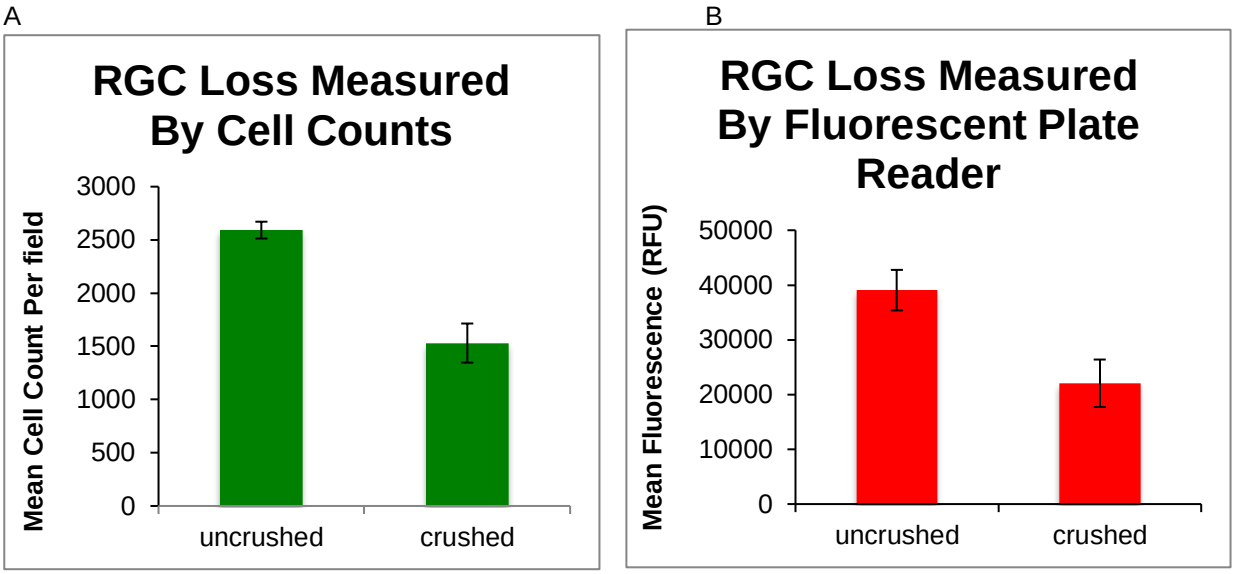

Figure 2. Optic nerve crush was performed on the right eye of adult mice, which were sacrificed 6 days after surgery. Cell counts of immunostained retinal flatmount images (n=3) show a 41% loss of cells after crush (A). Fluorescent reads of retinal homogenates (n=4) show a 44% loss of signal following crush (B).

Effect of HIOC on RGC Survival after Optic Nerve Crush

We continued to use the severe optic nerve crush procedure in our initial test of TrkB activators in order to test efficacy against a severe injury and because of the variability associated with the less severe injury. In this experiment we tested N-[2-(5-hydroxy- 1H-indol-3-yl)ethyl]-2-oxopiperidine-3-carboxamide (HIOC), in the optic nerve crush model. As RGCs possess TrkB receptors, we hypothesize that administration of HIOC immediately around the time of optic nerve crush would allow more RGCs to survive the injury.

THY1-CFP mice were injected i.p. with 40 mg/kg HIOC or vehicle (20% DMSO in PBS) roughly one hour before receiving the optic nerve crush or transection procedure. Under anesthesia, each mouse had the right optic nerve crushed. The fellow eye was left as a control. Mice were allowed to recover and were injected once daily with HIOC or vehicle following surgery until sacrifice at post-op day 6. Retinas were immediately dissected and frozen. Retinal homogenates were prepared in RIPA buffer with a protease inhibitor cocktail. The relative levels of fluorescence were measured in the supernatant fractions.

The mean fluorescence from naïve retinas (in regular fluorescence units) was 37502 ± 937 (Figure 3). The mean fluorescence of crushed/transected vehicle retinas was 18564 ± 567 and that of HIOC-treated retinas was 18338 ± 826. We did not see protection associated with HIOC treatment. It is possible that the mice are metabolizing the drug too quickly to allow for sufficient TrkB activation or the dose was insufficient. WE subsequently investigated the effects of doses of HIOC up to 100 mg/kg, but still saw no protection (data not shown).

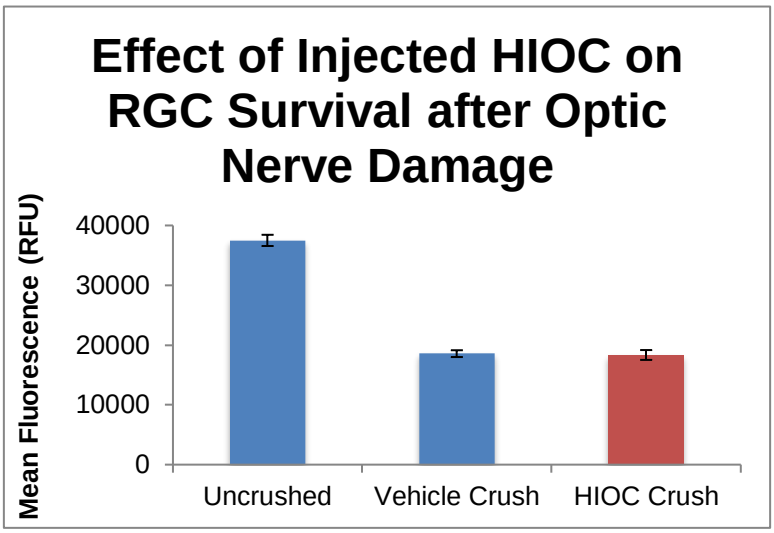

Figure 3. THY1-CFP mice received intraperitoneal injections of either 40 mg/kg HIOC or vehicle (20% DMSO in PBS) prior to receiving an optic nerve crush or transection to the right eye. Injections continued until 6 days after surgery, when mice were sacrificed. Retinas were homogenized and the fluorescence from each retina was quantified using a fluorescent plate reader.

To address a potential pharmacokinetic issue, we initiated the osmotic minipump experiments described in the proposal. C57BL6/J mice were pretreated with an intraperitoneal injection of HIOC (40 mg/kg) or vehicle, anesthetized and subjected to unilateral optic nerve crush. Each mouse then received a subcutaneous implant of an Alzet Model 2001 osmotic minipump containing HIOC or vehicle (40% DMSO). The HIOC concentration used provided a calculated drug delivery rate of 20 mg/kg/day. After six days, the mice were euthanized and the numbers of Brn3a-immunoreactive retinal ganglion cells (RGC) were determined in retinal flat mounts. Optic nerve crush caused a significant reduction in RGC number in both the vehicle and HIOC-treated mice ($p<0.01$, Figure 4). While the RGC number was slightly higher in the crushed HIOC-treated eye than in the crushed vehicle-treated eye, the effect was not statistically significant.

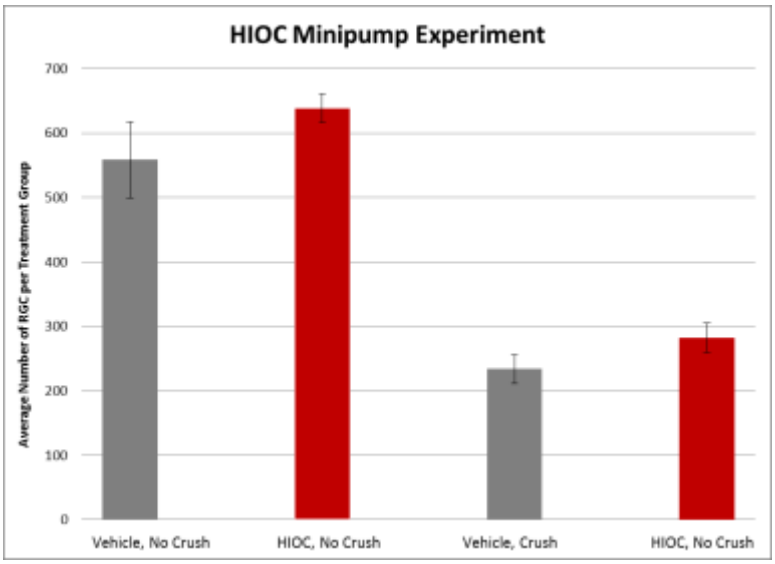

Figure 4. Effect of HIOC on optic nerve crush-induced retinal ganglion cell death. HIOC or vehicle were deliver via Alzet osmotic minipumps. Nerve crush significantly reduced RGC number ($p<0.01$), but HIOC did not significantly protect the cells from injury.

A similar result was observed with minipumps and quantification of fluorescent RGCs of Thy1-CFP mice (data not shown).

Effects of TrkB agonists Deoxygedunin and LM22A-4

Deoxygedunin is a naturally occurring compound that has been shown to activate TrkB receptors in the mouse brain (Jang et al., 2010). We sought to test the effectiveness of deoxygedunin in protecting RGCs against apoptosis following optic nerve crush. Five C57BL/6J mice from Jackson Laboratories were given an intraperitoneal injection of 5 mg/kg deoxygedunin and 4 were given vehicle (34% DMSO in PBS). Pharmacokinetic studies have shown that deoxygedunin is active two hours after administration. Therefore, injections were staggered so that each mouse received the optic nerve crush two hours after the initial injection. The right eye was operated on with the left eye serving as a control. Injections of deoxygedunin or vehicle were given daily until 6 days post-surgery when the mice were sacrificed. Eyes were enucleated, and retinas

immunostained for the RGC marker Brn-3a. The cell counts from vehicle and deoxygedunin-treated eyes that received crush decreased by 41% and 38.2%, respectively when compared to uncrushed eyes (Figure 8, $p<0.01$). We did not detect a protective drug effect with deoxygedunin at the dose tested. As with our other drug studies, we may need to investigate the pharmacokinetics of this agent to see if our dosing regimen needs to be altered in order to provide protection.

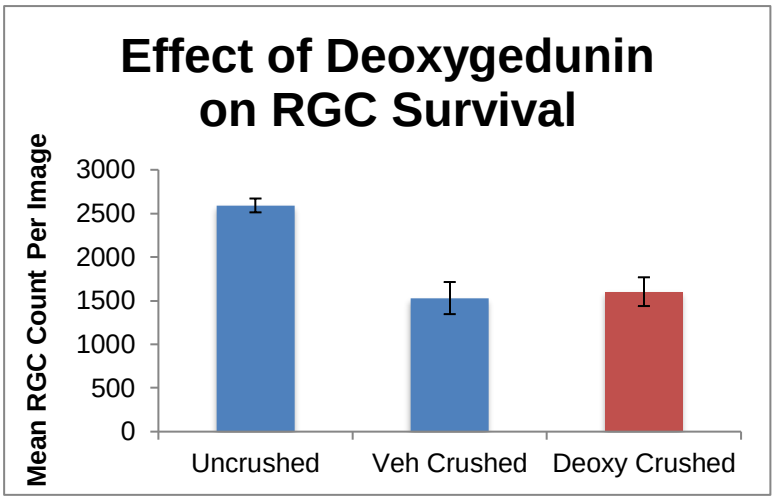

Figure 5. Mice received intraperitoneal injections of either 5 mg/kg deoxygedunin or vehicle (34% DMSO in PBS) prior to receiving an optic nerve crush to the right eye. Injections continued until 6 days after surgery, when mice were sacrificed. Retinas were immunostained for the RGC marker Brn-3a and imaged with a confocal microscope. RGCs were quantified using Cell Profiler software. Nerve crush significantly reduced the number of RGCs ($p<0.01$). Deoxygedunin did not significantly prevent cell loss.

We also examined the effects of another TrkB agonist, LM22A-4 (Massa et al., 2010). It also failed to protect RGCs following optic nerve crush (data not shown).

We have concluded that TrkB activation is not viable approach to rescue RGSs following optic nerve crush.

3B. Specific aim 2. To examine the ability of TrkB activators to prevent traumatic blast-induced retinal damage and loss of visual function.

To begin specific aim 2, we constructed and calibrated a blast gun, modeled after the one developed by Tonia Rex. A picture of the gun is shown in Figure 6.

Fig. 6. A miniature cannon for blast-induced trauma to the eye. The apparatus consists of a paintball gun (1) (without paintballs) with a customized barrel (2), a tube to hold the mouse (3), and a Honeywell pressure transducer to calibrate the force of the pressure wave (4).

Characterization of the effects of ocular blast on the retina and visual function.
To begin to characterize the effect of blast to the eye on the retina, we delivered a single blast of ~46 psi (range 45-47) to the left eye of 18 mice (14 Thy1-CFP and 4 wild type C57BL/6 mice). All mice survived the first week following blast. Seven of the mice were euthanized at 1 week for an initial assessment of retinal anatomy. We are examining flat mounted retinas and retinal sections for Thy1-CFP, Iba1 (microglia), and glial fibrillary acid protein (GFAP). Figure 7 shows the effects of blast injury at 7 days on Thy-CFP fluorescence. Blast induced a significant increase in fluorescence (see Struebing et al., 2017). In addition, we observed swelling of the RGC cell bodies.

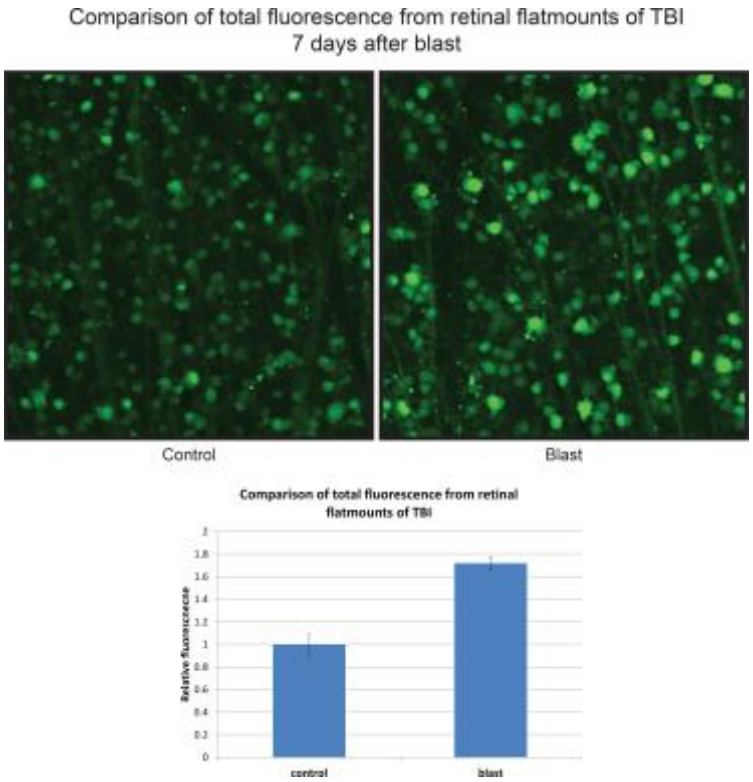

Figure 7. Effect of blast-induced injury on Thy-CFP fluorescent RGCs.

These changes were accompanied by an increase in Iba1-immunopositive microglia (Fig. 8), suggestive of an inflammatory response to blast, and an increase in GFAP, indicative of reactive gliosis.

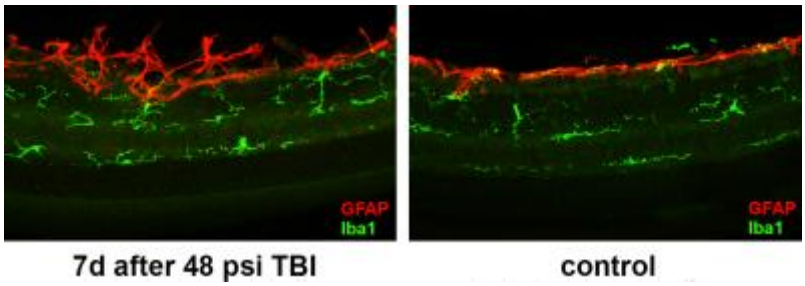

Fig. 8. Representative sections of retinas following 48 psi blast immunostained for GFAP (red) and Iba1 (green).

Surprisingly, this effect was accompanied by a significant decrease of Thy 1 mRNA in the retinas of mice with blast injury (Fig. 9). This suggests that the increase in Thy1-GFP fluorescence measured 1 week after blast may be due to impaired metabolism / proteolysis in the RGCs.

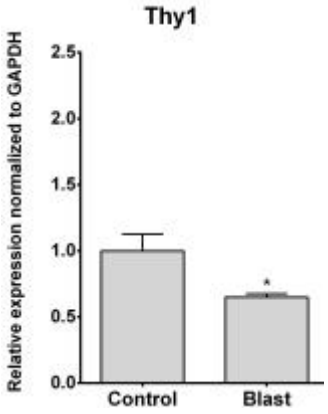

Fig. 9. Thy1 mRNA measured by quantitative reverse transcription-polymerase chain reaction (qRT-PCR)in retinas of controls and mice 1 week after exposure to ~46 psi blast. Blast injury was associated with a significant decrease in Thy1 mRNA ($p<0.05$).

Optokinetic tracking was used to assess contrast sensitivity at 1-2 weeks after exposure to a single ~46 psi blast. Contrast sensitivity was significantly reduced in blasted eyes compared to control at spatial frequencies of 0.064, 0.092, and 0.103 cycles / degree (c/d) (Figure 10). This indicates that the loss of visual function occurs rapidly after blast injury.

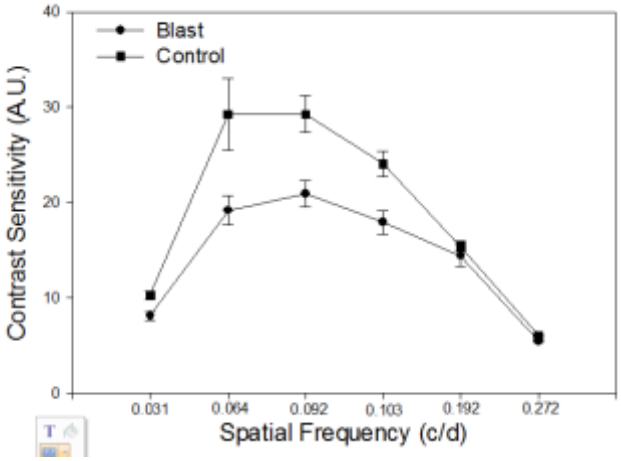

Figure 10. Contrast sensitivity functions measured 1-2 weeks after exposure to ~46psi blast. Contrast sensitivity was reduced in the eyes exposed to blast at 0.064, 0.092, and 0.103 c/d ($p<0.01$, N=8).

Dark-adapted electroretinogram (ERG) recordings were performed 8 weeks after exposure to blast (Figure 11). There was no decrease in either a-wave or b-wave amplitudes in the mice exposed to blast compared to controls. To the contrary, there was a trend towards higher a-wave and b-wave amplitudes. This result suggests that the impaired contrast sensitivity is due to inner retinal damage.

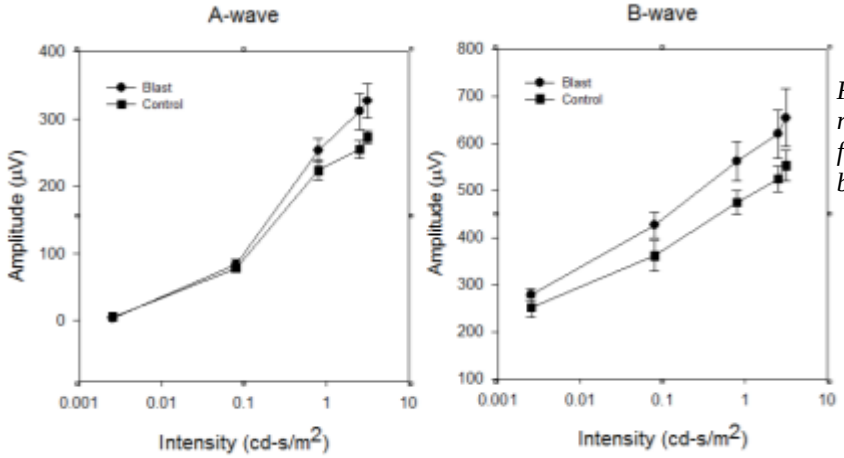

Figure 11. Dark-adapted ERG recordings measured 8 weeks following exposure to ~46 psi blast. N=4.

Consistent with this hypothesis, two months after exposure to blast, the outer retina of mice exposed to blast injury looked relatively normal; although morphometric analysis of the images remains to be done, there appears to be loss of RGCs and thinning of the inner plexiform later (Figure 12). In flat mounted retinas, a statistically significant reduction in Thy1-CFP retinal ganglion cells was observed in both the central and peripheral retina following blast injury (Figure13).

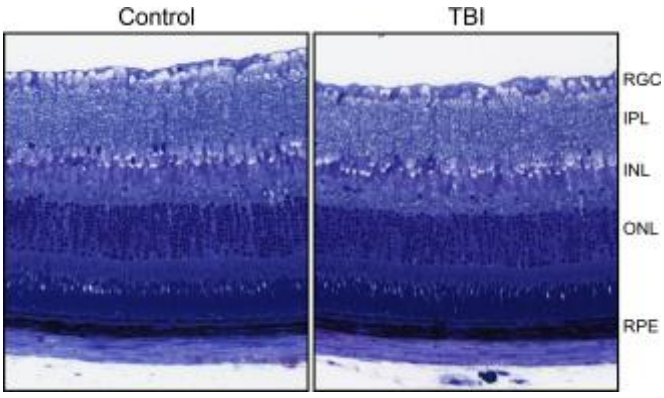

Figure 12. Morphology of the retina 2 months after blast injury. Representative 5μm plastic sections of retina from control mice and mice exposed to blast. RGC, retinal ganglion cell layer; IPL, inner plexiform layer; INL, inner nuclear layer; ONL, outer nuclear layer; RPE, retinal pigment epithelium.

13A

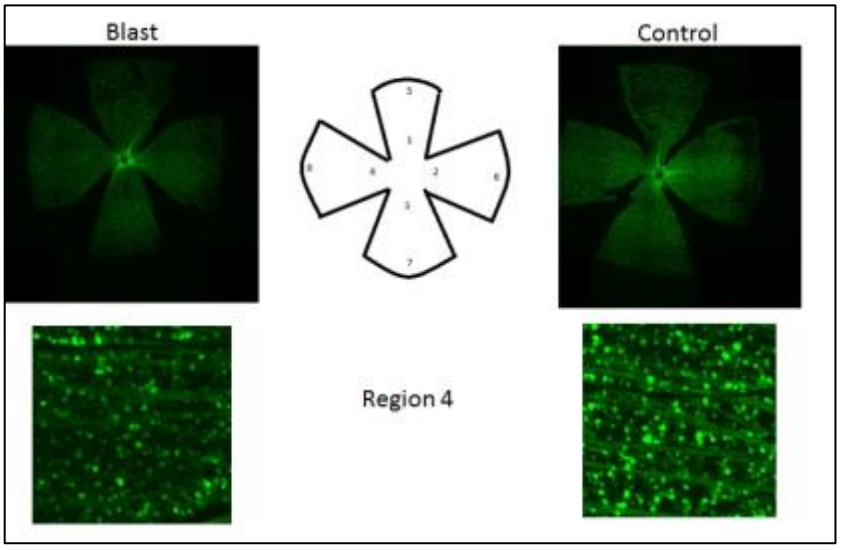

13B

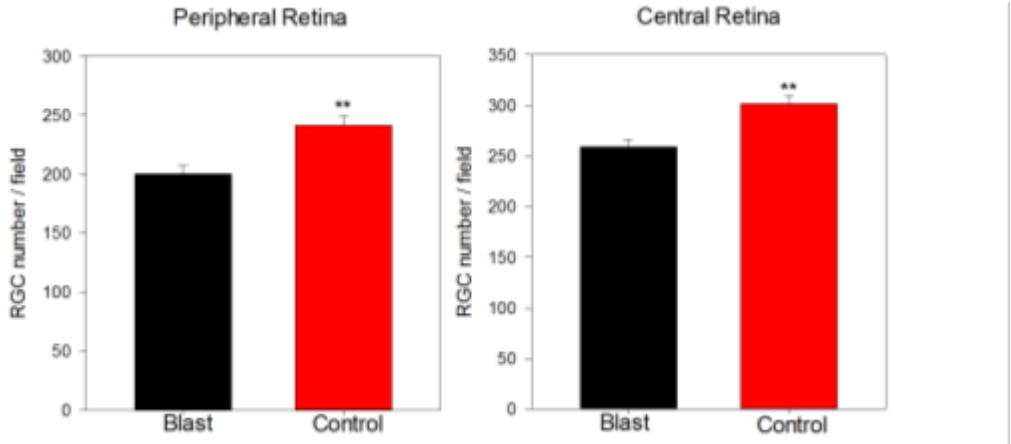

Figure 13. Retinal ganglion cell numbers were reduced two months after exposure to ~46psi blast. A. Representative images of flat mounted retinas showing Thy1-CFP retinal ganglion cells. B. Retinal ganglion cells were counted in eight 636.5 x 636.5 μm fields from each flat mounted retina. N=3-4; p<0.02.

Effect of HIOC on the contrast sensitivity deficit of mice exposed ~46 psi blast injury.

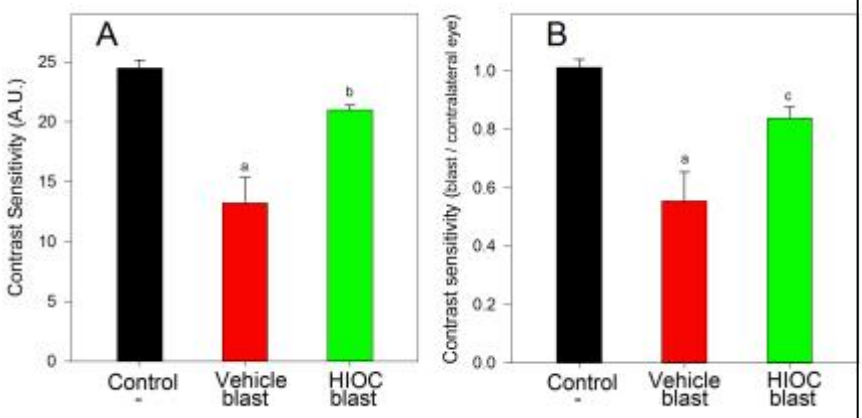

Figure 14. HIOC protects visual function from blast-induced injury. Mice were treated with HIOC (40 mg/kg, ip) on the day of blast exposure and daily for 1 week. Blast was delivered to the right eye of the Vehicle and HIOC groups. A separate untreated control group, not exposed to blast or drugs, was included. Contrast sensitivity was measured on the 8th day. Comparing left and right eye or blast to untreated control gave comparable results. Blast significantly decreased contrast sensitivity in the vehicle-treated mice ([a]P<0.001). HIOC significantly reduced the blast-induced decrease in contrast sensitivity ([b]P<0.01; [c]P<0.05).

We developed a new method to synthesize gram quantities of HIOC

(Setterholm et al., 2015). Thy1-CFP mice were treated with 40 mg/kg of HIOC on the day of blast and daily for 1 week. In this experiment, a separate control group that was not exposed to blast was included in order to compare the use of the contralateral eye of the blast mice as control *vs* a naïve control. In this experiment, exposure to blast caused a 46% decrease in contrast sensitivity in the vehicle treated blast eye group *vs* the naïve control, and only a 14% decrease in the HIOC treated mice (Figure 14A). HIOC significantly protected from blast-induced loss of function ($p<0.001$). A very similar result was observed when using the contralateral eye as control (Figure 14B; Vehicle, 45%; HIOC 17%).

We also tested LM22A-4, another TrkB activator (Massa et al., 2010), under similar conditions, and found that it also reduced the decrease of contrast sensitivity following blast injury to the eye ($p<0.05$; data not shown). However, it was not as effective as HIOC at mitigating the effects of blast injury to the eye. Therefore, we focused our attention on HIOC.

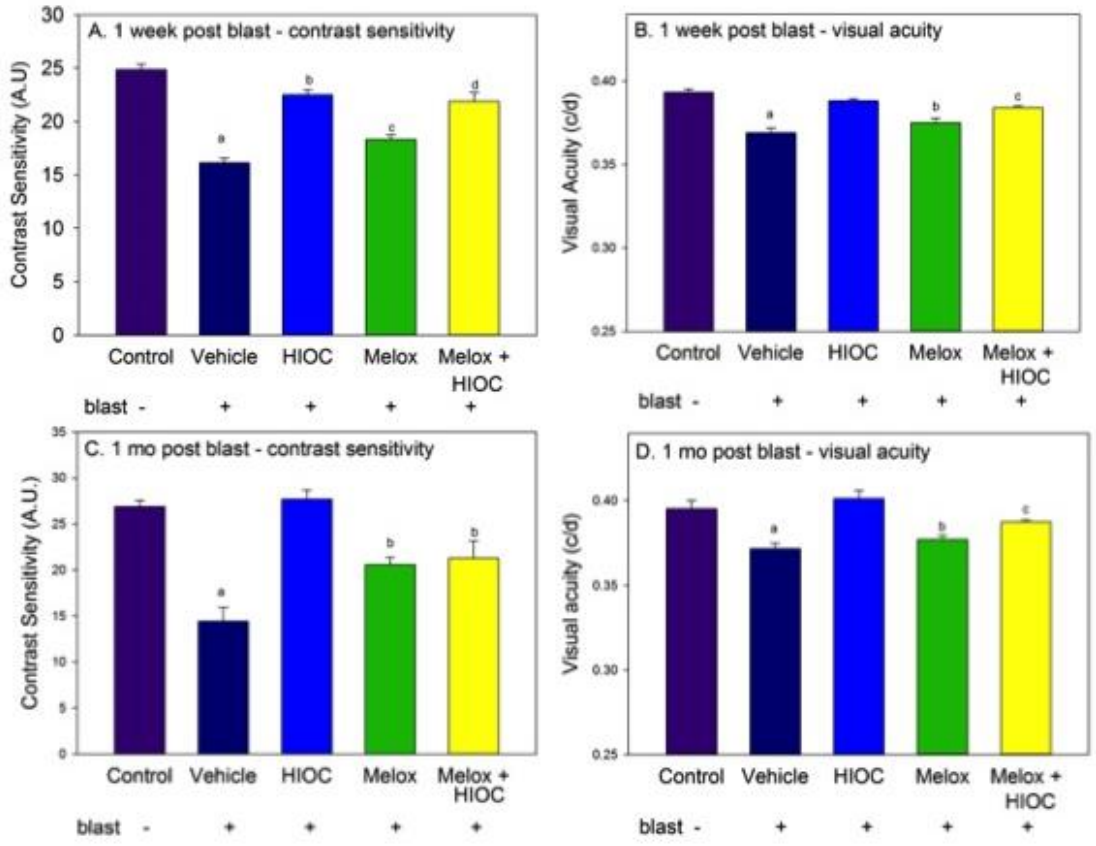

Figure 15. Effect of HIOC and meloxicam (Melox) on loss visual function following blast injury to the eye. *Mice were exposed to single ~48 psi blast directed to the eye. They were treated daily with HIOC (40 mg/kg ip), meloxicam (5 mg/kg sc), the two drugs together, or vehicles for 7 days beginning on the day of blast injury or vehicles. A separate, uninjured group (Control) was included for comparison. Visual function was tested 1 week and 1 month after injury. A. Contrast sensitivity 1 week after injury; N=6-8. a) Control vs Vehicle, $p<0.001$; b) HIOC vs Vehicle $p<0.001$, vs Control $p<0.05$; c) Meloxicam vs Vehicle $p<0.05$, Meloxicam vs HIOC and vs Control, $p<0.001$; Meloxicam + HIOC vs Control $p<0.01$, vs Vehicle $p<0.001$, vs HIOC not significant (NS), vs Meloxicam $p<0.001$. B. Visual acuity 1 week after injury; N=6-8. a)Vehicle vs Control $p<0.001$, vs HIOC $p<0.001$; b) Meloxicam vs Control $p<0.001$, vs HIOC $p<0.01$, vs Vehicle NS; c) Meloxicam + HIOC vs Control $p<0.05$, vs Vehicle $p<0.001$, vs HIOC NS, vs Meloxicam NS. C. Contrast sensitivity 1 month after injury; N=6-7. a) Vehicle vs Control $p<0.001$, vs HIOC $p<0.001$; Meloxicam or Meloxicam + HIOC vs Control $p<0.01$, vs Vehicle $p<0.01$. D. Visual acuity 1 month after injury; N=6-7. a)Vehicle vs Control $p<0.001$, vs HIOC $p<0.001$; b) Meloxicam vs Control $p<0.001$, vs HIOC $p<0.01$, vs Vehicle NS; c) Meloxicam + HIOC vs Control $p<0.05$, vs Vehicle $p<0.01$, vs HIOC NS, vs Meloxicam NS.*

Blast injury to the eye is associated with microglial activation and reactive gliosis (Fig. 8), indicative of inflammatory reactions. We therefore sought to examine the possible benefit of a combination of HIOC and anti-inflammatory drugs or immune modulators in the treatment of traumatic blast injury to the eye. Thy1-CFP mice were exposed to a single ~48 psi blast directed to the eye and treated with vehicle, the TrkB activator HIOC (40

mg/kg ip), the non-steroidal anti-inflammatory drug meloxicam (5mg/kg sc), or a combination of the two drugs. Drugs were administered for 1 week beginning on the day of blast. Visual function (contrast sensitivity and visual acuity) was assessed by optokinetic tracking (OKT) 1 week and 1 month after blast injury (Figure 15). Exposure to blast reduced contrast sensitivity, measured at a spatial frequency of 0.064 cycles/ degree (c/d), by 35 % and 46 % in the vehicle-treated mice at 1 week and 1 month, respectively (Fig. 15 A, C; $p<0.001$). HIOC partially reversed the loss of contrast sensitivity at 1 week and completely reversed the loss at 1 month ($p<0.001$). Meloxicam alone had a small, but significant protective effect at both time points, but the effect was significantly less than that of HIOC alone ($p<0.01$). The combined effect of HIOC and meloxicam was no more effective that HIOC alone at 1 week, and was significantly less effective than that of HIOC alone at 1 month. Similar trends were observed when measuring visual acuity (Fig. 15B, D), although the effects were smaller in all groups, as observed previously. We conclude that the 40 mg/kg dose of HIOC causes nearly complete recovery of function from the blast injury. Meloxicam alone had a small protective effect against blast injury, and that meloxicam in combination with HIOC is no more beneficial than HIOC alone under these conditions. It remains to be determined if it might potentiate the effect of a lower dose of HIOC or provide better protection from retinal ganglion cell (RGC) death.

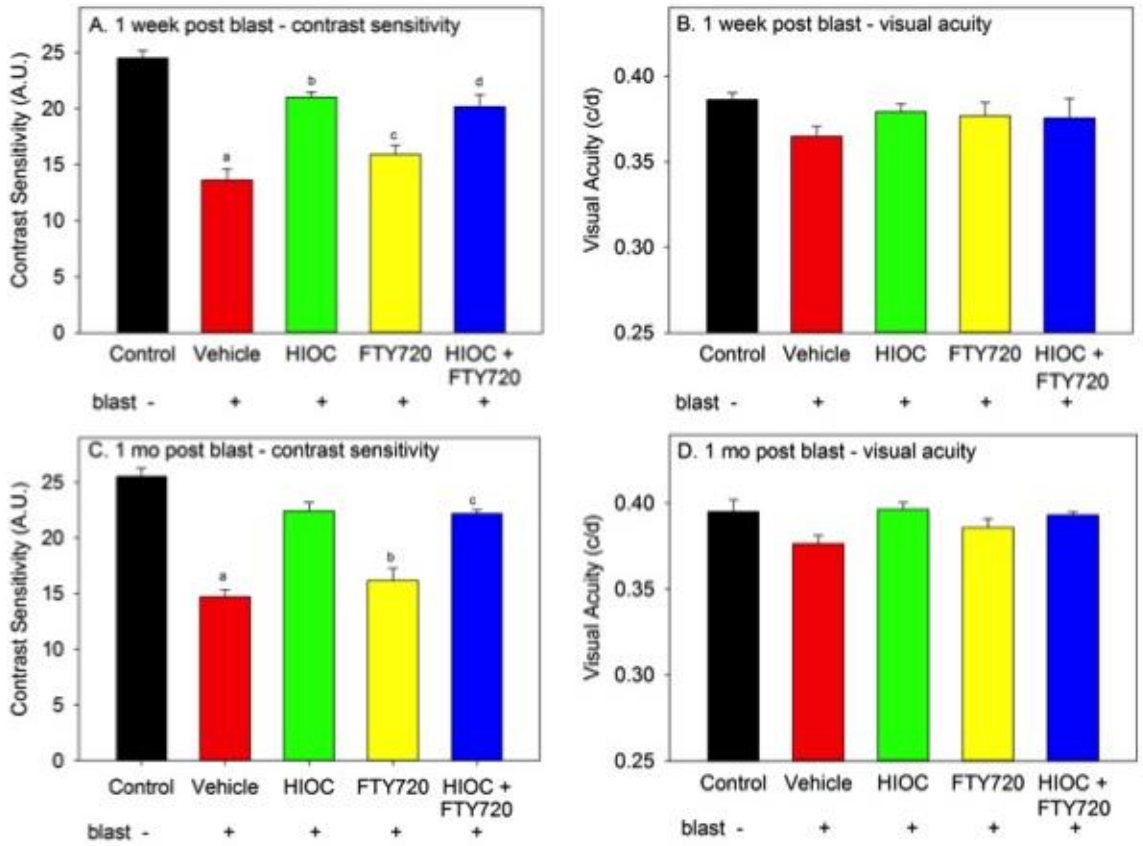

Figure 16. Effect of HIOC and FTY720 on loss visual function following blast injury to the eye*. Mice were exposed to single ~48 psi blast directed to the eye. They were treated daily with HIOC (40 mg/kg ip), FTY720 (10 mg/kg ip), the two drugs together, or vehicles for 7 days beginning on the day of blast injury or vehicles. A separate, uninjured group (Control) was included for comparison. Visual function was tested 1 week and 1 month after injury. A. Contrast sensitivity 1 week after injury; N=6. a) Vehicle vs Control p<0.001; b) HIOC vs Control p<0.01; vs Vehicle p<001; c) FTY720 vs Control p<0.001, vs Vehicle NS, vs HIOC p<0.001; d) HIOC + FTY720 vs Control p=0.001, vs Vehicle p<0.001, vs HIOC NS; vs FTY720 p=0.001. B. Visual acuity 1 week after injury; N=6. No significant differences. C. Contrast sensitivity 1 month after injury; N=6. a) Vehicle vs Control p<0.001, vs HIOC p<0.001; b) FTY720 vs Control p<0.001, vs Vehicle NS, vs HIOC p<0.001; d) HIOC + FTY720 vs Control p<0.05, vs Vehicle p<0.001, vs HIOC NS, vs FTY720 p<0.001. D. Visual acuity 1 month after injury; N=6. No significant differences.*

The effect of FTY720 (fingolimod), alone and in combination with HIOC was tested. FTY720 is a sphingosine 1-phosphate receptor agonist that reduces neuroinflammation in part by switching microglia to a neuroprotective phenotype and by inhibiting lymphocyte migration; it has shown clinical efficacy in the treatment of stroke and multiple sclerosis patients (Noda et al., 2013; Yang et al., 2014; Fu et al., 2014). Mice were exposed to a single ~48 psi blast directed to the eye and treated with vehicle, HIOC (40 mg/kg ip), FTY720 (10mg/kg ip), or a combination of the two drugs. Drugs were administered for 1 week beginning on the day of blast. Visual

function (contrast sensitivity and visual acuity) was assessed 1 week and 1 month after blast injury (Figure 16). Exposure to blast reduced contrast sensitivity, measured at a spatial frequency of 0.064 cycles/ degree (c/d), by 44 % and 42 % in the vehicle-treated mice at 1 week and 1 month, respectively. FTY720 alone did not significantly improve contrast sensitivity in the mice exposed to blast. HIOC significantly reduced the loss in contrast sensitivity to 15% and 12% at 1 week and 1 month, respectively. HIOC and FTY720 together provided no additional protection over HIOC alone under these conditions. A similar trend was observed when measuring visual acuity, but the effects were not statistically significant.

Defining the optimal time window for initiating HIOC treatment following exposure to a 48psi blast.

In all previous experiments, HIOC was administered 30 minutes prior to exposure to blast. This protocol effectively preserved visual function, as assessed by optokinetic tracking (OKT) measurement of contrast sensitivity. In this experiment, we determined if administration of HIOC 15 minutes to 24 hours after blast would also be effective. HIOC (40 mg/kg ip) or vehicle were administered for 1 week beginning on the day of blast. Visual function (contrast sensitivity and visual acuity) was assessed 1 week and 4 months after blast injury (Figure 17). Exposure to blast reduced contrast sensitivity, measured at a spatial frequency of 0.064 cycles/ degree (c/d), by 51 % and 55 % in the vehicle-treated mice at 1 week and 4 months, respectively. HIOC administered before blast injury partially reversed the loss of contrast sensitivity at 1 week ($P<0.05$) and completely reversed the loss at 4 months ($p<0.001$). HIOC administered 15 minutes, 1 hour, or 3 hours after blast injury was as effective as the drug administered before injury; contrast sensitivity of those treated with HIOC before blast was not statistically different from contrast sensitivity of mice administered HIOC 15, 60 or 180 minutes after blast ($p>0.2$). Visual acuity was not significantly affected one week after blast injury (data not shown). Four months after blast, visual acuity was reduced in the blast vehicle group (Figure 17; $p<0.001$). HIOC treatment showed an effect on visual acuity that was similar to that observed on contrast sensitivity.

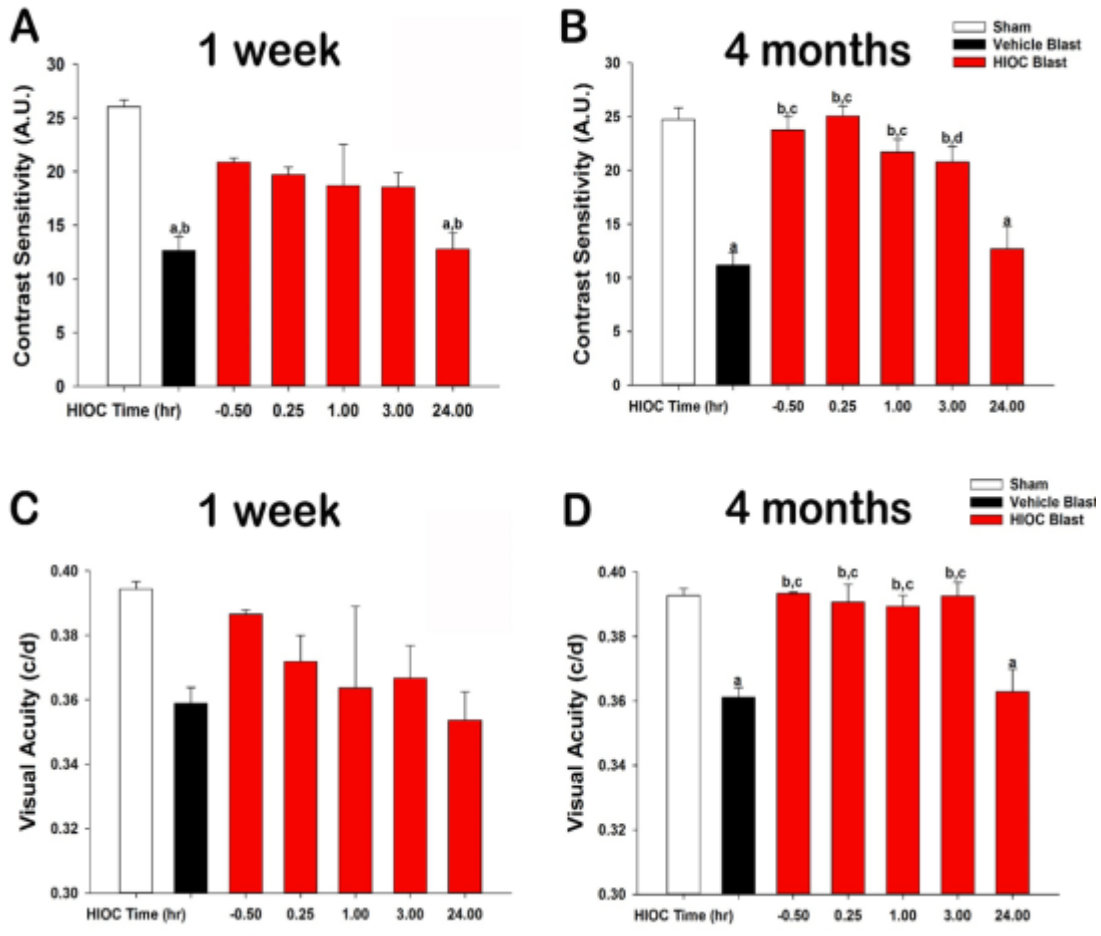

Figure 17. Effect of HIOC, administered before or after exposure to 48psi blast, on visual acuity and contrast sensitivity, assessed 4 months after blast injury*. Mice were exposed to single ~48 psi blast directed to the eye. They were treated with HIOC (40 mg/kg ip), 0.5 hour before blast or 0.25, 1, 3 or 24 hours after blast. Vehicle was administered 0.5 hours before blast. A separate, uninjured group (*Naïve*) was included for comparison. HIOC and vehicle were subsequently injected daily for an additional 6 days. Visual function was*

tested 4 months after injury. A. Contrast sensitivity 1 week: a) p<0.001 vs. Sham; b) p<0.05 vs HIOC at -0.05, 0.25, 1, and 3 hours. B. Contrast sensitivity 4 months: a) p<0.001 vs Sham; b) p<0.001 vs Vehicle and HIOC 24 hours; c) not significant (p>0.2) vs Sham. N=5-6.

These data indicate that HIOC, administered for 1 week, can prevent or reduce the loss visual function if it is administered with 3 hours of blast injury. The effect of the therapy was greater 4 months after blast than one week, suggesting that following one week of treatment functional recovery continues and vision improves.

Effect of HIOC, administered after ~48psi blast, on retinal ganglion cell loss.

Thy1-CFP mice were exposed to a single ~48psi blast and were injected with vehicle or HIOC (40 mg/kg ip) 15 minutes later. The mice were then injected with vehicle or HIOC daily for the next 6 days. After 4 months, mice were euthanized and retinal flat mounts were prepared. Fluorescent retinal ganglion cells were counted in eight fields, 4 in central retinal and 4 in peripheral retina. As reported previously, blast caused a small reduction in retinal ganglion cells (RGCs) (Figure 18). The effect was statistically significant only in peripheral retina (p<0.05). HIOC administration significantly preserved RGCs in peripheral retina (p<0.05). Similar trends were obsserved in central retina, but they were not statistically significant.

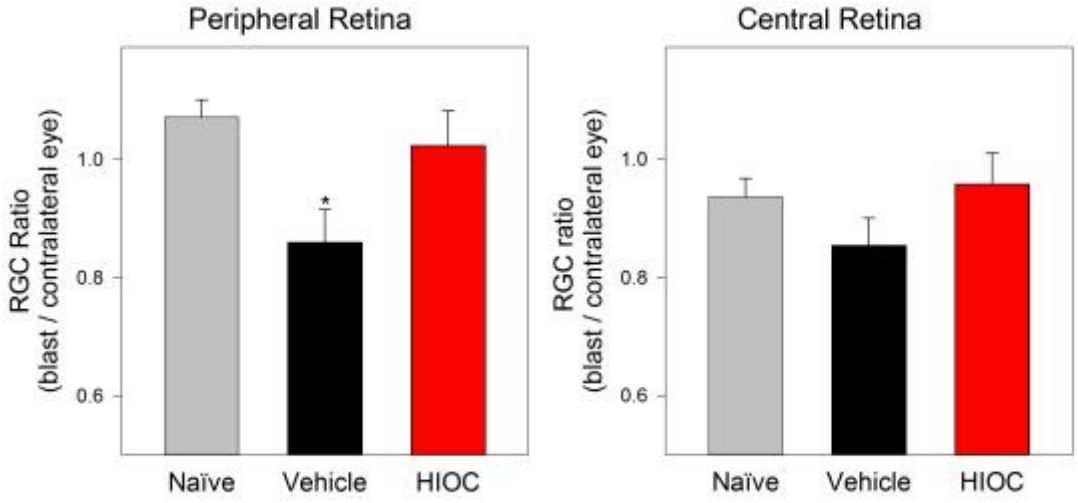

Figure 18. Effect of HIOC, administered after exposure to 48 psi, on retinal ganglion cell loss*. Mice were exposed to single ~48 psi blast directed to the right eye. They were treated with HIOC (40 mg/kg ip) or vehicle 15 min later. A separate, uninjured group (*Naïve*) was included for comparison. HIOC and vehicle were subsequently injected daily for an additional 6 days. Four months after exposure to blast, fluorescent RGCs were counted in eight fields, 4 in central retinal and 4 in peripheral retina. Data are expressed as a ratio of the RGCs in between the right (blast) and left (contralateral) eyes, normalized to account for inter-animal differences in numbers of fluorescent RGCs. *p<0.05 vs Naïve and vs HIOC blast. N=6 / group.*

Effect of blast directed at the eye on optic nerve axon survival; mitigation by HIOC.

Mice were exposed to ~48psi blast to the right eye and treated with HIOC (40 mg/kg, i.p.) or vehicle 15 minutes later; a separate, naïve control group was included for comparison. Treatment continued daily for the next 6 days. Mice were euthanized four months later; optic nerves were dissected, embedded in plastic and sectioned.

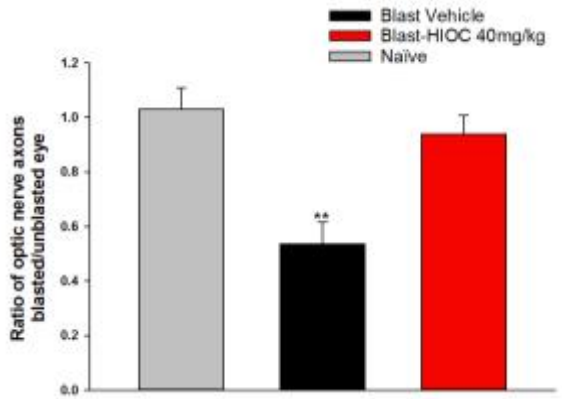

Optic nerve axons were counted as described in Templeton et al. (2014). Blast caused a 46% reduction in axons in the vehicle-treated mice (**p<0.01), but no significant decrease in axons in the HIOC treated mice (Fig. 10, Fig. 19, 20).

Figure 19. Effect of 48 PSI blast with and without HIOC on optic nerve axon numbers. *Data are expressed as a ratio of the axon numbers in the optic nerve of the right eye, exposed to blast overpressure, divided by the number of*

axons in the left, contralateral eye of each mouse. N=6 per group.

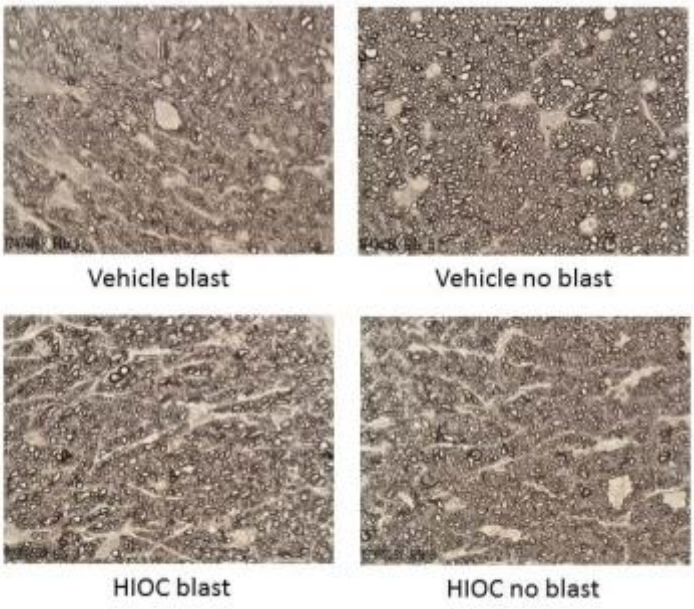

Figure 20. Representative photomicrographs of optic nerves from vehicle-treated or HIOC-treated mice. *On the left are the nerves of eyes exposed to blast; on the right are the nerves from the contralateral eyes of the same mice. Note the loss of axons in the optic nerve of the vehicle treated mouse, but not of the HIOC treated mouse.*

<u>Does HIOC preserve visual function by stimulating BDNF / TrkB receptors?</u>

We previously showed that HIOC stimulates TrkB, resulting in its phosphorylation and activation of downstream signaling (Shen et al., 2012), but it is unknown if the efficacy of the drug in preventing blast-induced vision loss occurs through this mechanism. Towards the end of Q3 FY2015, we initiated a study to explore the mechanism. ANA12 is a selective TrkB antagonist that binds to the receptor and inhibits downstream signaling (Cazarola et al., 2011). We tested the ability of ANA12 to block the protective action of HIOC. The results suggested that ANA12 blocked the beneficial effect of HIOC on visual function. However, the blast-induced decrease in visual function was less than typically observed in previous experiments, and the beneficial effect of HIOC was smaller than usual. We therefore repeated the experiment. Mice were exposed to a single ~48 psi blast and administered HIOC (40 mg/kg ip) or vehicle15 min later. Daily injections continued for 6 days. Mice were pretreated with ANA12 (0.5 mg/kg ip) or its vehicle 2.5 hours before each HIOC / vehicle injection. One month after exposure to blast, contrast sensitivity and visual acuity were reduced in the vehicle-treated mice (Figure 21; $p<0.001$). Treatment with HIOC (plus the vehicle for ANA12) reduced the loss of contrast sensitivity ($p<0.001$). Administration of ANA12 alone had no effect on the blast-induced loss of contrast sensitivity, but completely blocked the effect of HIOC. The results indicate that HIOC mitigates blast-induced vision loss by activating TrkB.

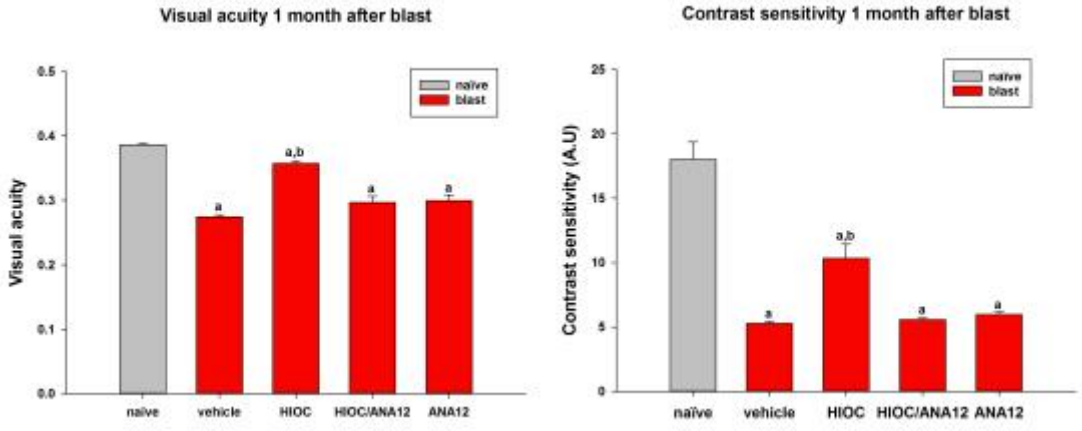

Figure 21. Effect of ANA12 on the mitigation of blast-induced vision loss by HIOC*. See text for details. N=6 / group. a) p<0.001 vs Naïve; b) p<0.001 vs Vehicle, ANA12, and HIOC/ANA12.*

Optic nerve axon counts from this experiment showed that blast injury caused ~35% loss of optic nerve axons in vehicle-treated mice measured 5 weeks after blast (Figure 22; p<0.013). HIOC nearly completely prevented this axon loss. ANA12 appeared to partially block the effect of HIOC, as there was no significant difference between the axon numbers of mice receiving ANA12 alone and ANA12 plus HIOC. However, there was no significant difference between HIOC alone and ANA12 plus HIOC.

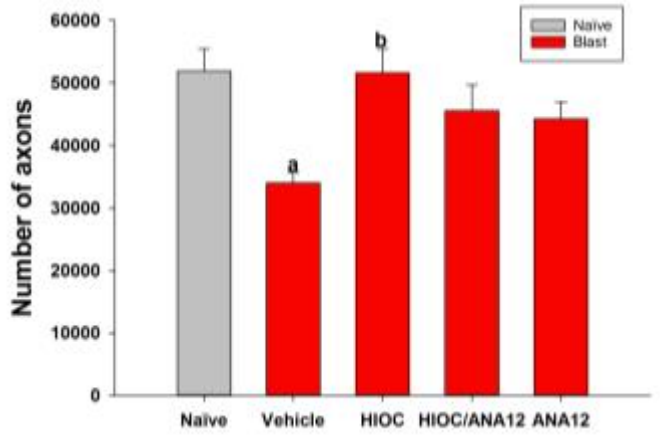

Figure 22. Effect of ANA12 on the mitigation of blast-induced optic nerve axon loss by HIOC*. See text for details. N=5-6 / group. a) p<0.013 vs Naïve; b) p<0.014 vs Vehicle.*

Effect of HIOC on ocular blast-induced GFAP expression in the retinal ganglion cell layer.

Glial fibrillary acidic protein (GFAP) is a marker of astrocytes, and is expressed in Müller glial cells when the outer retina is damaged. We previously reported that 48 psi blast directed at the front of the eye caused an upregulation of glial fibbrillary acidic protein (GFAP) in astocytes in the nerve fiber and ganglion cell layer, but not in Müller glial cells. In this study, we exammined the effect of HIOC (40 mg/kg, i.p.) on this response. Mice were subjected to a single blast at 48 psi. HIOC or vehicle was injected 15 min after blast, and once daily for the next 6 days. Eyes were dissected 7 days after blast. As shown in the representative images in Figure 23, exposure to blast caused an increase of GFAP expression, indicative of gliosis in the nerve fiber layer and ganglion cell layer. Consistent with our previous results, there was no apparent increase in GFAP in Müller cell processes in the inner plexiform or inner nuclear layers. HIOC produced an obvious reduction GFAP expression in the eyes exposed to blast. To quantify the changes of GFAP, the average length of GFAP-labeled processes was measure in nerve fiber and ganglion cell layers of peripheral and central retina (Figure 24). Blast significantly increased GFAP process length in the peripheral retina (p<0.05), and this effect was significantly reversed by HIOC treatment. A similar trend was observed in the central retina, but it was not statistically significant due to increased variability. The results suggest that blast induces reactive astrocytosis, and that treatment with HIOC reduces this effect. This may contribute to the preservation of visual function by HIOC.

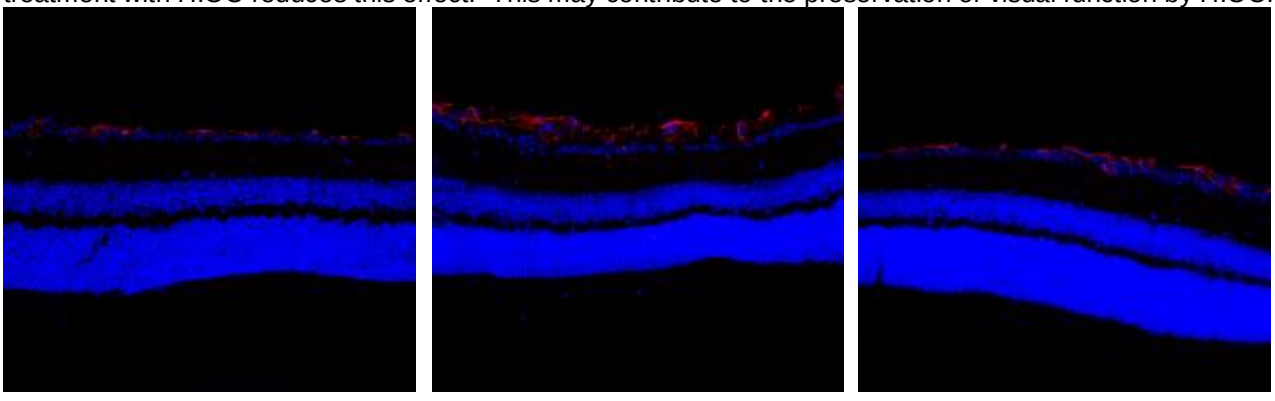

Figure 23. HIOC reduces the induction of gliosis caused by ocular blast.
Representative images of GFAP labeling (red) in mice exposed to 48 psi blast, treated with vehicle or HIOC (40 mg/kg, i/p.). Sample sizes: Sham 3, Vehicle 6, HIOC 5. Blue labeling is the nuclear stain DAPI.

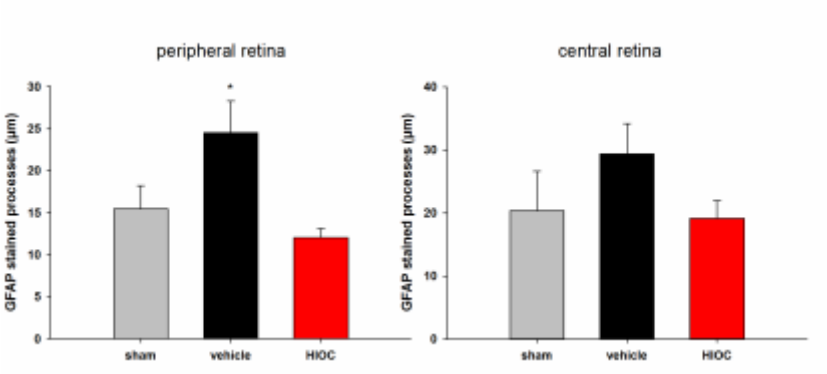

Figure 24. Quantification of average GFAP process length in the nerve fiber layer and GCL. *Mice were exposed to 48 psi blast, treated with vehicle or HIOC (40 mg/kg, i/p.). Retinas were stained for GFAP immunoreactivity 7 days after blast. Sample sizes: Sham 3, Vehicle 6, HIOC 5. *p<0.05.*

Effect of HIOC on blast-induced Iba1-labeled microglia.

Mice were treated as described above. Retinal sections were stained for Iba1. Representative sections are shown in Figure 25. Image analysis was performed to assess microglial activation. The samples are still being imaged, but preliminary observations suggest that HIOC reduces blast-induced microglial activation (see Figure 5).

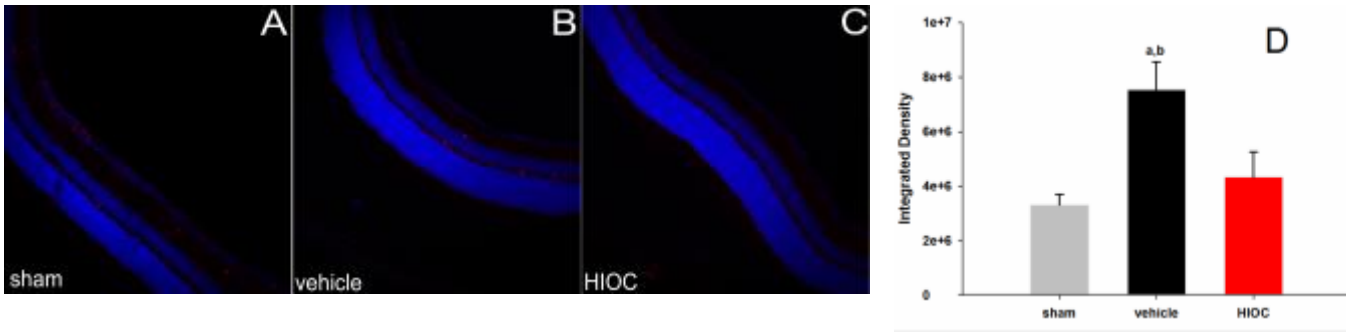

Figure 25. Effect of HIOC on ocular blast-induced microglial activation in the retina. *Representative images of Iba 1 labeling (red) in mice exposed to 48 psi blast, treated with vehicle or HIOC (40 mg/kg, i/p.). Blue labeling is the nuclear stain DAPI. A. sham; B. blast + vehicle; C. blast + HIOC; D. quantification of Iba1 staining density of amoeboid-shaped microglia using Image-J. N=3-4. a) p<0.02 vs sham; b) p<0.05 vs HIOC.*

SD-OCT measurements of retina following blast directed at the eye.

Spectral-domain optical coherance tomography (SD-OCT) was used to assess effects of blast on retinal layers 1 day and 7 days after 48 psi blast, in mice treated with vehicle or HIOC as described above. One day after blast, no significant changes in total retinal thickness, photoreceptor layer thickness, or ganglion cell / nerve fiber layer thickness were observed (data not shown). However, 7 days after blast there was a statistically significant reduction in ganglion cell / nerve fiber layer thickness in the vehicle-treated, blast-exposed mice (Fig. 26; $p<0.001$). Other retinal layers were unaltered. Treatment with HIOC (40 mg/kg) significantly reduced the loss of ganglion cell / nerve fiber layer thickness caused by ocular blast (Fig. 26; $p<0.01$).

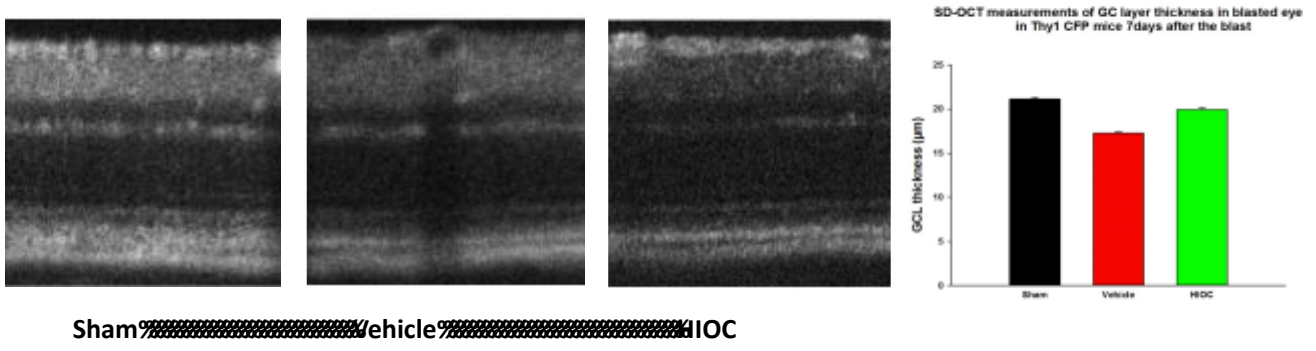

Figure 26. Ocular blast reduces ganglion cell / nerve fiber layer thickness: protection by HIOC. N=6 per group.

Specific Aim 3B. To examine the ability of HIOC to preserve visual function resulting from traumatic brain injury.

Effect of different blast pressures directed at the head on visual function. To further characterize the effects of blast directed at the head, we compared the effects of 50 psi and 70 psi blast pressure. Mice were exposed to single blast directed at the right side of the head. Visual function was tested one and two weeks after blast exposure. Contrast sensitivity was reduced more at 2 weeks (Fig. 28) than at 1 week (Fig. 27) for both pressures. For visual acuity, no significant reduction was observed at 1 week after exposure, but significant reductions were observed at 2 weeks. These observations are indicative of a progressive loss of visual function following head blast. With both blast pressures, the loss of contrast sensitivity detected through the right eye was reduced more than that detected through the left eye when measured two weeks after blast exposure ($p<0.001$), and the effect of 70psi blast pressure was significantly greater than that of 50 psi ($p<0.001$; Fig. 28). A similar pattern was observed for loss of visual acuity at 2 weeks, where acuity detected through the right eye was significantly worse than through the left eye following 70 psi blast ($p<0.001$), but not following 50 psi blast (Fig. 28). Similar to contrast sensitivity, 70 psi caused a greater loss of visual acuity compared to that observed with 50 psi ($p<0.001$ right eye; $p<0.05$ left eye). In view of these results we have chosen to use 70 psi blast in all future experiments because of the more robust loss of visual function compared to 50 psi.

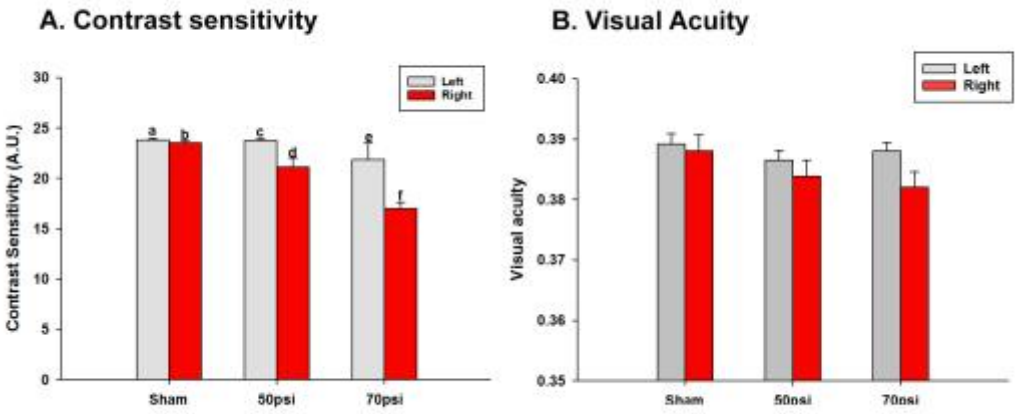

Figure 27. Comparison of different blast pressures measured 1 week after exposure. *Mice were treated as described above.* ***Contrast sensitivity:*** *a vs b, c, and e, not significant; b vs d, $p<0.05$; b vs f, $p<0.001$; d vs f, $p<0.005$; c vs d, $p<0.05$; e vs f, $p<0.001$.* ***Visual acuity:*** *no significant differences. N=6 mice per condition.*

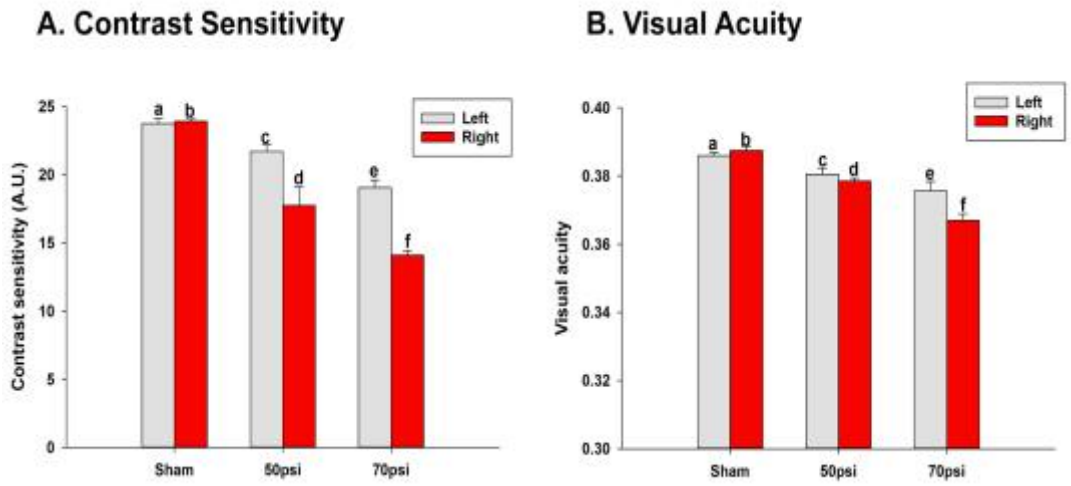

Figure 28. Comparison of different blast pressures measured 2 weeks after exposure. *Mice were treated as described above.* ***Contrast sensitivity:*** *a vs b, not significant; a vs c; p<0.05; a vs e, p<0.001; b vs d and f, p<0.001; d vs f, p<0.001; c vs d, p<0.001; e vs f, p<0.001.* ***Visual acuity:*** *a vs b, not significant; a vs c, not significant; a vs e, p<0.001; b vs d and f, p<0.001; d vs f, p<0.001; c vs d, not significant; e vs f, p<0.001. N=6 mice per condition.*

Effect of blast overpressure directed at the side of the head on cerebral microglia

Mice were exposed to a single ~70 psi blast to the side of the head (TBI). Brain sections, prepared 21 days after blast exposure, were immunostained for Iba1 to label microglia. We observed microglial activation in the cortex of the blasted side of the brain (Figure 29).

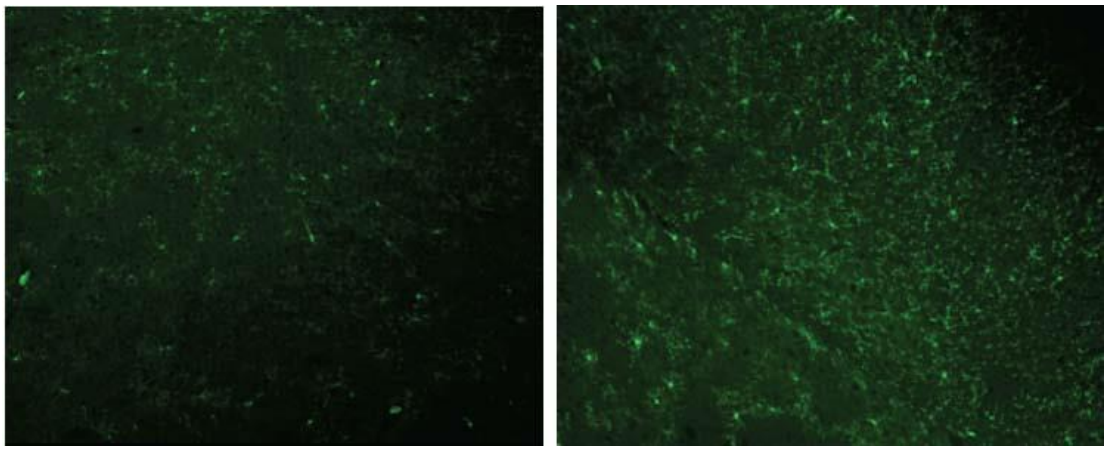

Naïve **21 days post-TBI**

Figure 29. Representative Iba1 immunostained brain section from naïve mice and mice exposed to blast directed at the side of the head (TBI).

Effect of HIOC on vision loss from blast directed at the side of the head.

We tested the efficacy of HIOC in treating the loss of visual function from blast overpressure directed at the side of the head (Figure 30). Mice were exposed to a single blast of ~70 psi directed on the right side of the head. Visual acuity and contrast sensitivity were measured seperately for right and left eyes. Blast directed at the right side of the head resulted in decrease in contrast sensitivity mediated through both eyes (p<0.001), indicative of bilateral brain damage. However, the loss of visual function was greater ipsilateral to the blast (p<0.001). HIOC (40 mg/kg, ip), administered for the first week after blast, significantly reduced the loss of contrast sensitivity and visual acuity when measured one month after the blast (p<0.001).

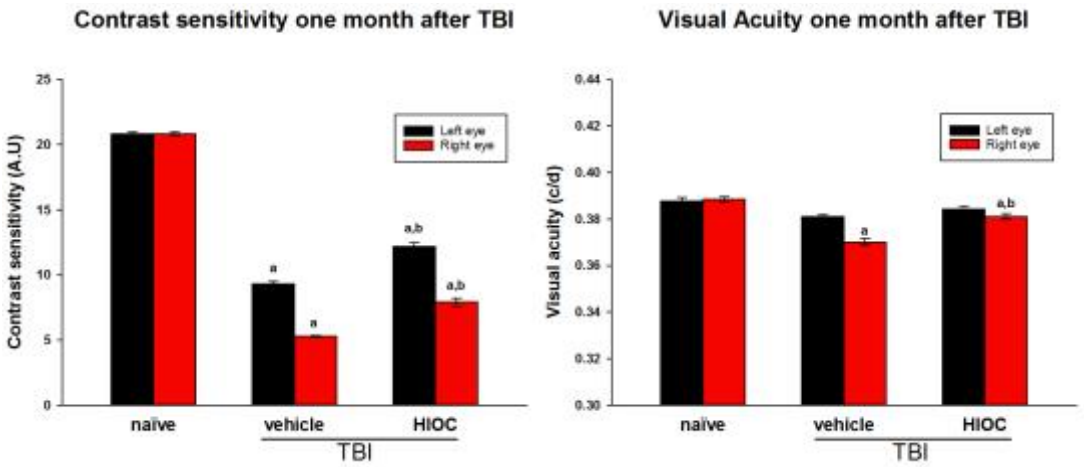

Figure 30. Effect of HIOC on the loss of visual function from head trauma.
Mice were exposed to a single ~70psi blast directed at the right side of the head. HIOC (40mg/kg i.p.) or vehicle was administered 15 minutes after exposure to blast, and daily for the next six days. A naïve control group was included for comparison. Visual acuity and contrast sensitivity were tested one month after exposure to blast. Head trauma significantly decreased contrast sensitivity and visual acuity ([a]p<0.001 vs Naïve; n=6/group), with a geater decrement in visual function mediated by the right eye ([b]p<0.001 vs Vehicle left; n=6/group). HIOC partially prevented this loss of visual function [c]p<0.001 vs Vehicle; n=6/group).

Because the protective effect of HIOC at 40 mg/kg was relatively small, we tested additional doses, ranging from 10-80 mg/kg, examining contrast sensitivity and visual function mediated through the right eye (Figure 31). Mice were exposed to a single blast of ~70 psi directed on the right side of the head. Visual acuity and contrast sensitivity were measured 1 week after blast. At 10 mg/kg, HIOC had no protective effect. At 40 mg/kg, HIOC had a small protective effect, simar in magnitude to that shown in Figure 30. At 80 mg/kg, the highest dose tested, HIOC completed prevented the loss of TBI-induced visual dysfunction (p<0.001 for contrast sensitivity and p<0.01 for visual acuity).

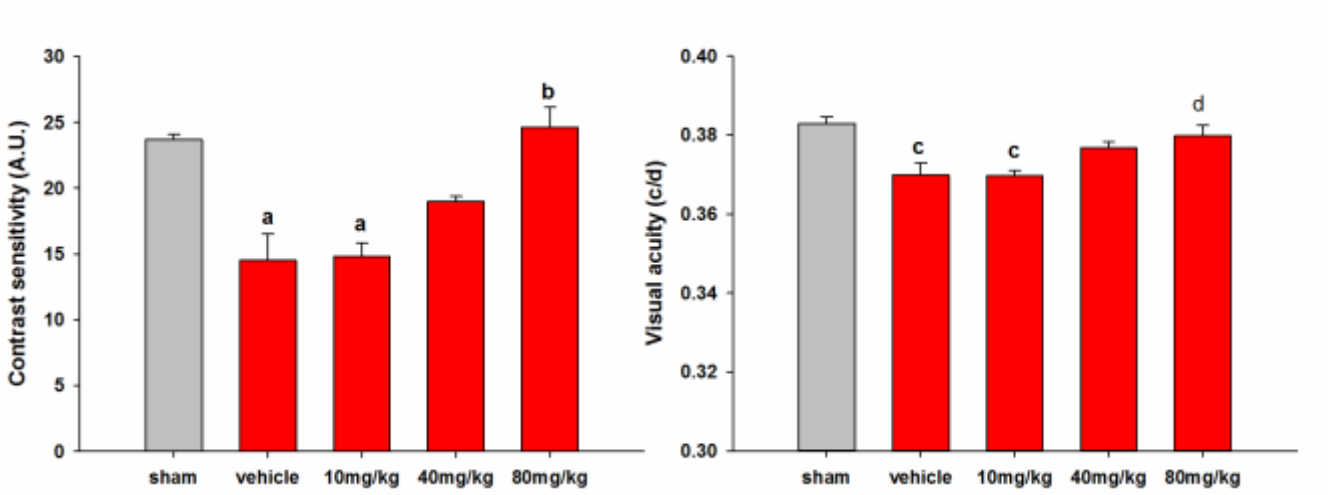

Figure 31. Effect of HIOC on TBI-induced loss of visual function: dose-response. *Mice were exposed to a single ~70psi blast directed at the right side of the head. HIOC or vehicle was administered 15 minutes after exposure to blast, and daily for the next six days. A naïve control group was included for comparison. Visual function was tested 1 week after blast. [a]p<0.001 vs sham; [b]p<0.001 vs vehicle and 10 mg/kg; [c]p<0.01 vs sham; [d]p<0.01 vs vehicle and 10 mg/kg. N=5-6 per group.*

4. KEY RESEARCH ACCOMPLISHMENTS

- HIOC reduces the loss of visual function following blast injury to the eye or the head.

- The protective effect of HIOC is dose dependent
- HIOC reduces the induction of astrocyctosis in the ganglion cell and nerve fiber layers from ocular blast.
- HIOC reduces the thinning of the ganglion cell / nerve fiber layers caused by ocular blast.
- The neuroprotective effect of HIOC involves activation of BDNF / TrkB receptors.

5. CONCLUSIONS

Our results indicate that HIOC preserves visual function and optic nerve axons following blast injury to the eye. HIOC reduces loss of visual function following blast injury to the head. The mechanism of action of HIOC involves activation of BDNF / TrkB receptors. HIOC may be useful for preventing vision loss in soldiers exposed to blast overpressure.

6. PUBLICATIONS, ABSTRACTS, AND PRESENTAIONS

a. Publications

1. Lay press: none

2. Peer-reviewed scientific journals:

Setterholm, N.A., McDonald, F.E., Boatright, J.H., Iuvone, P.M.: Gram scale, chemoselective synthesis of *N*-[2-(5-hydroxy-1H-indol-3-yl)ethyl]-2-oxopiperidine-3-carboxamide (HIOC). Tetrahedron Lett., 56: 3413–3415, 2015. http://dx.doi.org/10.1016/j.tetlet.2015.01.167; PMID: 26028783; PMC4445863.

Struebing F, King R, Li Y, Chrenek M, Lyuboslavsky P, Sidhu C, Iuvone PM, Geisert E. Transcriptional changes in the mouse retina following ocular blast injury: A role for the immune system. J. Neurotrauma, 2017 Jun 9. https://doi.org/10.1089/neu.2017.5104; [Epub ahead of print]; PMID: 28599600.

Dhakal S, Lyuboslavsky P, He L, Sidhu C, Struebing FL, Boatright JH Geisert EE, McDonald, FE, Sutterholm NA, Iuvone PM. Closed-globe trauma to the eye causes loss of visual function and optic nerve degeneration: Protection by HIOC through a BDNF/TrkB receptor mechanism. In preparation.

Iuvone PM, Dhakal S, Brock J, He L, Lyuboslavsky P. The BDNF/TrkB activator HIOC preserves vision in mouse model of traumatic brain injury. In preparation.

Foster S, Chrenek M, Iuvone PM, Boatright JH. A novel method for rapid quantification of mouse retinal ganglion cell loss. In preparation.

3. Invited articles:

Nothing to report

b. Abstracts and Presentations

Boatright JH, Foster S, Chrenek M, Iuvone M. Novel metrhod for deteremining retinal ganglion cell loss. Poster Abstract 16, ISER Glaucoma Symposium.

Chrenek, Micah A.; Sellers, Jana; Foster, Stephanie L.; Iuvone, P M.; Boatright, Jeffrey H. Novel method for quantifying loss of retinal ganglion cell in mice. ARVO eAbstract 397, 2014.

Scott, Jessica and Iuvone, P Michael. TrkB agonists for the treatment of traumatic vision loss. 14th Annual Rabb-Venable Excellence in Research Program, National Medical Association Ophthalmology Section.

Setterholm, N.A., McDonald, F.E., Boatright, J.H., Iuvone, P.M.: Gram scale, chemoselective synthesis of *N*-[2-(5-hydroxy-1H-indol-3-yl)ethyl]-2-oxopiperidine-3-carboxamide (HIOC). Tetrahedron Lett., 56: 3413–3415, 2015. http://dx.doi.org/10.1016/j.tetlet.2015.01.167; PMID: 26028783; PMC4445863.

Sidhu C., Lyuboslavsky P., Chrenek M. Struebing F.L., Sellers J.T., Setterholm N.A., McDonald F.E., Boatright J.H., Geisert E.E., Iuvone P.M.: Traumatic blast-induced injury reduces visual function and retinal ganglion cells of Thy1-CFP mice: Mitigation by a small molecule TrkB activator. Association for Research in Vision and Ophthalmolgy, eAbstract 6032-B0211, 2015.

Iuvone PM, Lyuboslavsky, P Sidhu C, He L, Boatright JH, Geisert EE. Protection from blast-induced vision loss by the N-acetylserotonin derivative HIOC through a BDNF/TrkB receptor mechanism. Association for Research in Vision and Ophthalmolgy, eAbstract 737-B0370, May 2016.

Iuvone PM, Dhakal S, Lyuboslavsky P, He L, Struebing FL, Boatright JH Geisert EE. HIOC, a TrkB receptor activator, for the treatment of blast-induced vision loss. XXII Biennial Meeting of the International Society for Eye Research, September 2016.

Iuvone PM, Dhakal S, Lyuboslavsky P, He L, Struebing FL, Boatright JH, Geisert EE. Closed-globe trauma to the eye causes loss of visual function and optic nerve degeneration: Protection by the N-acetyltryptamine derivative HIOC through a BDNF/TrkB receptor mechanism. XVII International Symposium on Retinal Degeneration, September 2016.

Iuvone PM, Dhakal S, Lyuboslavksy PN, He L, and Geisert EE. Loss of visual function following blast-induced ocular trauma and TBI: Protection by HIOC through a BDNF/TrkB receptor mechanism. 6th Military Vision Symposium on Ocular and Vision Inury. Boston, MA. March 2017.

7. INVENTIONS, PATENTS AND LICENSES

Nothing to report

8. REPORTABLE OUTCOMES

Nothing to report

9. OTHER ACHIEVEMENTS

Organized and spoke at a symposium at the XXII Biennial Meeting of the International Society for Eye Research, "TBI (traumatic brain injury): visual dysfunction and treatment."

10. REFERENCES

Cazorla M, Prémont J, Mann A, Girard N, Kellendonk C, Rognan D. (2011) Identification of a low-molecular weight TrkB antagonist with anxiolytic and antidepressant activity in mice. J Clin Invest 121:1846-57.

Feng G., Mellor R.H., Bernstein M., Keller-Peck C., Nguyen Q.T., Wallace M., Nerbonne J.M., Lichtman J.W., and Sanes J.R. (2000) Imaging Neuronal Subsets in Transgenic Mice Expressing Multiple Spectral Variants of GFP. Neuron 28 (1):41-51.

Fu Y., Zhang N., Ren L., Yan Y., Sun N., Li Y.J., Han W., Xue R., Liu Q., Hao J., Yu C., Shi F.D. (2014) Impact of an immunemodulator fingolimod on acute ischemic stroke. Proc Natl Acad Sci USA 111:18315-20.

Gauthier R., Joly S., Pernet V., Lachapelle P. and Di Polo A. (2005) Brain-Derived Neurotrophic Factor Gene Delivery to Muller Glia Preserves Structure and Function of Light-Damaged Photoreceptors. Investigative Ophthalmology Visual Science 46, 3383-3392.

Jang S. W., Liu X., Pradoldej S., Tosini G., Chang Q., Iuvone P. M. and Ye K. (2010a) N-acetylserotonin activates TrkB receptor in a circadian rhythm. Proc Natl Acad Sci U S A 107, 3876-3881.

Jang S. W., Liu X., Yepes M., Shepherd K. R., Miller G. W., Liu Y., Wilson W. D., Xiao G., Blanchi B., Sun Y. E. and Ye K. (2010b) A selective TrkB agonist with potent neurotrophic activities by 7,8-dihydroxyflavone. Proceedings of the National Academy of Sciences 107, 2687-2692.

Jang S. W., Liu X., Chan C. B., France S. A., Sayeed I., Tang W., Lin X., Xiao G., Andero R., Chang Q., Ressler K. J., and Ye K. (2010c) Deoxygedunin, a natural product with potent neurotrophic activity in mice. PLoS.One. 5 (7):e11528.

Massa S.M., Yang T., Xie Y., Shi J., Bilgen M., Joyce J. N., Nehama D., Rajadas J., Longo F. M. (2010) Small molecule BDNF mimetics activate TrkB signaling and prevent neuronal degeneration in rodents. J Clin Invest 120 (5):1774-85.

Mohan K, Kecova H, Hernandez-Merino E, Kardon RH, Harper MM. (2013) Retinal ganglion cell damage in an experimental rodent model of blast-mediated traumatic brain injury. Invest Ophthalmol Vis Sci 54: 3440-50.

Nadal-Nicolas F.M., Jiminez-Lopez M., Sobrado-Calvo P., Nieto-Lopez L., Canovas-Martinez I., Salinas-Navarro M. Vidal-Sanz M., and Agudo M. (2009) Brn3a as a marker of retinal ganglion cells: qualitative and quantitative time course studies in naive and optic nerve-injured retinas. Investigative Ophthalmology Visual Science 50 (8):3860-3868.

Noda H., Takeuchi H., Mizuno T., Suzumura A. (2013) Fingolimod phosphate protomotes the neuroprotective effects of microglia. J Neuroimmunol 256: 13-18, 2013.

Setterholm, N.A., McDonald, F.E., Boatright, J.H., Iuvone, P.M.: Gram scale, chemoselective synthesis of *N*-[2-(5-hydroxy-1H-indol-3-yl)ethyl]-2-oxopiperidine-3-carboxamide (HIOC). Tetrahedron Lett., 56: 3413–3415, 2015.

Shen J., Ghai K., Sompol P., Liu X., Cao X., Iuvone P.M., and Ye K. (2012) N-acetyl serotonin derivatives as potent neuroprotectants for retinas. Proceedings of the National Academy of Sciences 109 (9):3540-3545.

Templeton JP, Struebing FL, Lemmon A, Geisert EE. (2014) ImagePAD, a novel counting application for the Apple iPad, used to quantify axons in the mouse optic nerve. Exp Eye Res 128:102-8.

Weber A. J., Viswaníthan S., Ramanathan C. and Harman C. D. (2010) Combined Application of BDNF to the Eye and Brain Enhances Ganglion Cell Survival and Function in the Cat after Optic Nerve Injury. Investigative Ophthalmology & Visual Science 51, 327-334.

Yang D., Sun Y.Y., Bhaumik S.K., Li Y., Baumann J.M., Lin S.H., Dunn R.S., Liu C.Y., Shie F.S., Lee Y.H., Wills-Karp M., Chougnet C.A., Kallapur S.G., Lewkowich I.P., Lindquist D.M., Murali-Krisna K., Kuan C.Y. (2014) Blocking lymphocyte trafficking with FTY720 prevents inflammation-sensitized hypoxic-ischemic brain injury in newborns. J Neurosci. 34: 16467-81.

11. Personnel paid from this grant

P. Michael Iuvone, PhD
Jeffrey H. Boatright, PhD
Keqiang Ye, PhD
Li He, PhD
Susov Dhakal
Polina Lyuboslavsky
Curran Sidhu
Stephanie Foster
Leela (Sankaran) Geeter
Julien Brock
Fazila Aseem
Carlie Hoffman

Tetrahedron Letters 56 (2015) 3413–3415

Contents lists available at ScienceDirect

Tetrahedron Letters

journal homepage: www.elsevier.com/locate/tetlet

Gram-scale, chemoselective synthesis of *N*-[2-(5-hydroxy-1*H*-indol-3-yl)ethyl]-2-oxopiperidine-3-carboxamide (HIOC)

Noah A. Setterholm [a], Frank E. McDonald [a,*], Jeffrey H. Boatright [b,c], P. Michael Iuvone [b,d]

[a] Department of Chemistry, Emory University, 1515 Dickey Drive NE, Atlanta, GA 30322, USA
[b] Department of Ophthalmology, Emory University School of Medicine, 1365B Clifton Road NE, Atlanta, GA 30322, USA
[c] Rehabilitation R&D Center, Atlanta VA Medical Center, Decatur, GA 30033, USA
[d] Department of Pharmacology, Emory University School of Medicine, 1510 Clifton Road NE, Atlanta, GA 30322, USA

ARTICLE INFO

Article history:
Received 3 December 2014
Revised 22 January 2015
Accepted 26 January 2015
Available online 31 January 2015

In fond memory of Prof. Harry Wasserman, recognizing his humanity, scholarship, and service

Keywords:
Amide synthesis
Chemoselectivity
Decarboxylation
Kinase activation
Serotonin

ABSTRACT

N-[2-(5-Hydroxy-1*H*-indol-3-yl)ethyl]-2-oxopiperidine-3-carboxamide (HIOC) is a potent activator of the TrkB receptor in mammalian neurons and of interest because of its potential therapeutic uses. In the absence of a commercial supply of HIOC, we sought to produce several grams of material. However, a synthesis of HIOC has never been published. Herein we report the preparation of HIOC by the chemoselective *N*-acylation of serotonin, without using blocking groups in the key acylation step.

Introduction

Tropomyosin related kinase B (TrkB) is a neuronal transmembrane receptor protein in humans and other mammals. Small proteins such as brain-derived neurotropic factor (BDNF) bind to the extracellular portion of TrkB, triggering autophosphorylation of tyrosine residues in its intracellular domain. This phosphorylation then initiates cascade-signaling pathways known to promote neuronal differentiation and survival.[1] Several small molecules have been identified as agonists of Trk receptors,[2] including *N*-acetylserotonin (NAS, **2**, Fig. 1) as a TrkB activator.[3] In the course of investigating the TrkB activity of other serotonin derivatives, *N*-[2-(5-hydroxy-1*H*-indol-3-yl)ethyl]-2-oxopiperidine-3-carboxamide (HIOC, **3**) has displayed greater activation of TrkB, and exhibits a longer in vivo half-life than NAS.[4] HIOC has also demonstrated protective activity in an animal model for light-induced retinal degeneration, and can pass the blood-brain and blood-retinal barriers.[4] Thus, HIOC is a compound with high therapeutic potential, provided that this compound can be reliably prepared on a scale suitable for animal studies.

Although HIOC (**3**) is described in patents,[5] a method for its preparation has not been disclosed. Moreover, this compound is not consistently commercially available. Herein we describe a method for the gram-scale synthesis of HIOC.

At the first glance, HIOC would appear to be trivially prepared from the *N*-acylation of serotonin (Fig. 2). In practice, there are a number of plausible challenges:

(1) serotonin can undergo acylation at three sites;
(2) the carboxylic acid synthon **4** may potentially undergo decarboxylation upon standing; and
(3) serotonin-HCl **1** and the carboxylic acid **4** both exhibit poor solubility in most organic solvents.

Results and discussion

Carboxylic acid synthon **4** was prepared by basic hydrolysis of the commercially available ethyl ester **5**.[6,7] However, the literature did not provide a method for isolating this water-soluble

* Corresponding author.
E-mail address: frank.mcdonald@emory.edu (F.E. McDonald).

http://dx.doi.org/10.1016/j.tetlet.2015.01.167
0040-4039/

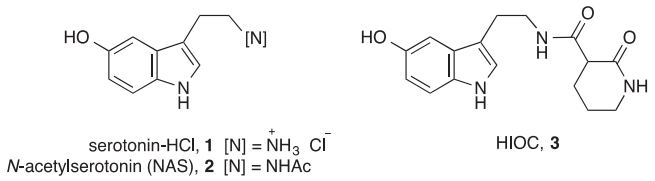

Figure 1. Structures of serotonin and derivatives, including HIOC (**3**).

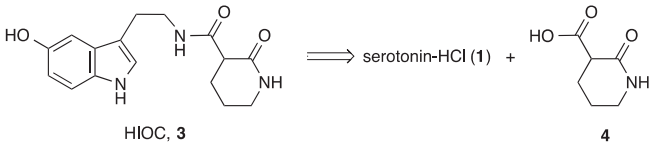

Figure 2. Retrosynthesis of HIOC.

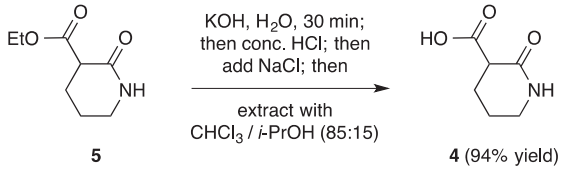

Scheme 1. Preparation and isolation of 2-oxo-3-piperidinecarboxylic acid (**4**).

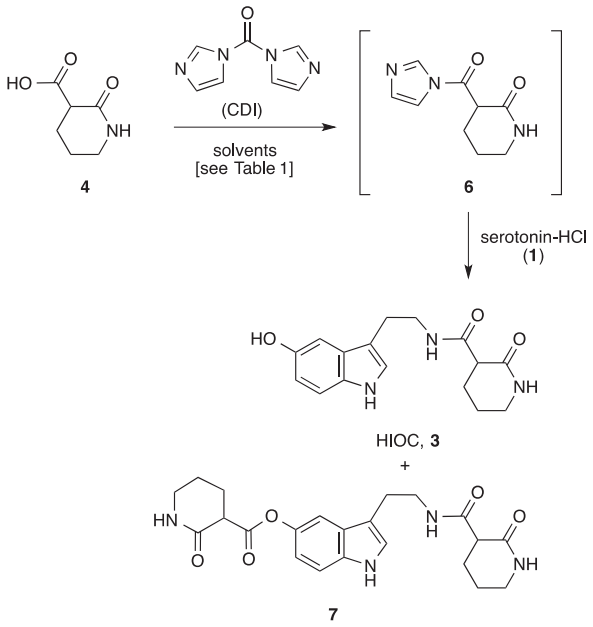

Scheme 2. Acylation of serotonin with carboxylic acid **4**.

compound. After some optimization we found that treatment of ester **5** with KOH in water, followed by addition of concentrated HCl and saturation of the aqueous layer with solid NaCl allowed for extraction of the desired acid **4** with a solvent mixture of chloroform and isopropanol (Scheme 1).[8]

We initially attempted to couple the carboxylic acid **4** with serotonin-HCl (**1**) by activating the acid using carbodiimide reagents[9] as well as through mixed anhydride formation.[10] In the case of the carbodiimide reagents, a small amount of HIOC was detected via LC–MS, but could not be isolated. Attempts to activate **4** with methyl chloroformate furnished the methyl ester of **4** as the only identifiable product. Efforts using pivaloyl chloride were also unsuccessful, resulting only in pivaloylation of the primary amine of serotonin. After screening additional methods we found that the carboxylic acid could be activated with carbonyl diimidazole (CDI).[11] Addition of CDI to an opaque suspension of carboxylic acid **4** in dichloromethane provided complete conversion to the soluble *N*-acyl imidazole derivative **6** (Scheme 2). Addition of serotonin-HCl (**1**) to intermediate **6** gave some conversion to the desired amide **3**. This acylation procedure was plagued by the poor solubility of serotonin-HCl in CH_2Cl_2, and *N*,*O*-bisacylated product **7** was often observed from these heterogeneous reaction conditions, along with some recovered unacylated serotonin. However, dimethylformamide (DMF) solubilized all reaction components, giving 66% conversion to HIOC (**3**) after 3 h, along with only 6% of the bisacylated product **7** (Table 1, entry 1). The product **3** was very difficult to extract from an aqueous acidic workup of the reaction mixture, so we sought an alternative to DMF as the solvent.

Adding an equal volume of triethylamine to the reaction mixture in CH_2Cl_2 prior to the addition of serotonin-HCl (**1**) gave some conversion to product, however the serotonin-HCl was not completely solubilized, leading to a small amount of bisacylated product **7** (entry 2). On the other hand, addition of an equal volume of pyridine (~40 equiv prior to addition of serotonin-HCl **1**) resulted in a completely homogeneous reaction mixture (entry 3). After 3 h, the reaction had proceeded to 66% conversion and high chemoselectivity favoring HIOC (**3**), with only a trace amount of

Table 1
Optimization of reaction conditions

Entry	Solvents	Conversion by ^{1}H NMR		
		Serotonin-HCl (**1**) (%)	HIOC (**3**) (%)	**7** (%)
1	DMF[a]	25	66	6
2	1:1 CH_2Cl_2/Et_3N[b]	68	29	3
3	1:1 CH_2Cl_2/pyridine[b]	33	66	<1

[a] CDI was added to a 0.3 M solution of **4** in DMF. After 30 min, another volume of DMF was added followed by 1 equiv of **1**.
[b] CDI was added to a 0.3 M suspension of **4** in CH_2Cl_2. After aging 30 min, an equal volume of base (triethylamine or pyridine) was added, followed by 1 equiv of **1**.

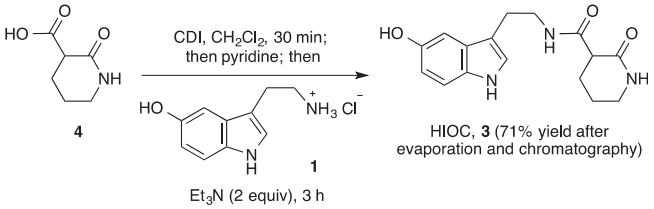

Scheme 3. Optimized acylation for the synthesis of HIOC (**3**).

N,*O*-bisacylated product detected by NMR.[12] The addition of 2 equiv of triethylamine helped to push the reaction to completion over the course of 3 h, bringing the conversion up to ~85% (Scheme 3). Isolation of the product from the reaction mixture was non-trivial. Concentration of the reaction mixture followed by dry loading of the unwieldy crude onto a silica gel column allowed for chromatographic separation with ethyl acetate/methanol (9:1) as eluent. The resulting solid was washed with hot diethyl ether to remove remaining imidazole impurities to furnish HIOC (**3**) in 71% yield (Scheme 3).

In summary, we have developed a short, scalable, and highly reproducible synthesis of HIOC without the need for protective groups. The key discovery was the utility of the additional volume of pyridine to the acyl-imidazole species, which helped to solubilize the serotonin hydrochloride and also may have behaved as a nucleophilic catalyst.

Acknowledgments

This work was financially supported by DOD W81XWH-12-1-0436, NIH R01EY004864, R01EY014026, P30EY006360, the Abraham J. and Phyllis Katz Foundation, and Research to Prevent Blindness (RPB). PMI is a recipient of the RPB Senior Scientific Investigator Award. We also thank Dr. Brooke Katzman (Emory University) for assistance with LC/MS.

Supplementary data

Supplementary data (experimental procedures, characterization data, ^{1}H and ^{13}C NMR spectra for 2-oxopiperidine-3-carboxylic acid (**4**) and HIOC (**3**)) associated with this article can be found, in the online version, at http://dx.doi.org/10.1016/j.tetlet.2015.01.167. These data include MOL files and InChiKeys of the most important compounds described in this article.

References and notes

1. (a) Kaplan, D. R.; Miller, F. D. *Curr. Opin. Neurobiol.* **2000**, *10*, 381–391; (b) Huang, E. J.; Reichardt, L. F. *Annu. Rev. Neurosci.* **2001**, *24*, 677–763.
2. (a) Obianyo, O.; Ye, K. *Biochim. Biophys. Acta* **1834**, *2013*, 2213–2218; (b) Webster, N. J. G.; Pirrung, M. C. *BMC Neurosci.* **2008**, *9*, S1.
3. Jang, S.-W.; Liu, X.; Pradoldej, S.; Tosini, G.; Chang, Q.; Iuvone, P. M.; Ye, K. *Proc. Natl. Acad. Sci. U.S.A.* **2010**, *107*, 3876–3881.
4. Shen, J.; Ghai, K.; Sompol, P.; Liu, X.; Cao, X.; Iuvone, P. M.; Ye, K. *Proc. Natl. Acad. Sci. U.S.A.* **2012**, *109*, 3540–3545.
5. (a) Tkachenko, S. E.; Okun, I. M.; Rivkis, S. A.; Kravchenko, D. V.; Khvat, A. V.; Ivashchenko, A. V. Russ. Pat. (2007) RU 2303597 C1 (CAN 147:181575). (b) Ran, R. Faming Zhuanli Shenqing (2012) CN 102816103 A (CAN 158:105451).
6. (a) Shapiro, D.; Abramovitch, R. A. *J. Am. Chem. Soc.* **1955**, *77*, 6690–6691; (b) Narayanan, K.; Cook, J. M. *J. Org. Chem.* **1991**, *56*, 5733–5736.
7. Compound **4** (2-oxo-3-piperidinecarboxylic acid) is listed in the Sigma–Aldrich catalog, CBR01770. We determined that a commercial sample (lot# B00037799) was merely valerolactam, corresponding to decarboxylation of compound **4**.
8. Continuous extraction of the salted aqueous layer with dichloromethane was also investigated, but tended to give reduced yields.
9. Basarab, G. S.; Jordan, D. B.; Gehret, T. C.; Schwartz, R. S. *Bioorg. Med. Chem.* **2002**, *10*, 4143–4154.
10. Yamada, K.; Teranishi, S.; Miyashita, A.; Ishikura, M.; Somei, M. *Heterocycles* **2011**, *83*, 2547–2562.
11. Paul, R.; Anderson, G. W. *J. Am. Chem. Soc.* **1960**, *82*, 4596–4600.
12. The diminished yield of bisacylated product **7** relative to HIOC (**3**) may arise from pyridine-promoted transacylation of serotonin-derived esters, although this has not been proven.

Journal of Neurotrauma

DOI: 10.1089/neu.2017.5104

Transcriptional Changes in the Mouse Retina Following Ocular Blast Injury: A Role for the Immune System

Felix L. Struebing[1,2], Rebecca King[1,3], Ying Li[1,4], Micah A. Chrenek[1,5], Polina N. Lyuboslavsky[1,6], Curran S. Sidhu[1,7], P. Michael Iuvone[1,8], Eldon E. Geisert[1*]

[1]Department of Ophthalmology, Emory University, Atlanta GA 30322

Running title: The Transcriptome of Ocular Blast Injury in Mice

Table of contents title: Transcriptional Changes in the Mouse Retina Following Ocular Blast injury

Address for all authors:

Emory University

1365B Clifton Rd NE

Room 5500

Atlanta, GA 30305 USA

Email for all authors:

[2] fstrueb@emory.edu, [3] rking2@emory.edu, [4] ying.li@emory.edu, [5] mchrene@emory.edu, [6] polina.n.lyuboslavsky@emory.edu, [7] curran.sidhu@emory.edu, [8] miuvone@emory.edu

[*]**Corresponding Author:**

Eldon E. Geisert

Department of Ophthalmology

Emory University

1365B Clifton Rd NE

Room 5500

Atlanta, GA 30305 USA

Email: egeiser@emory.edu

Phone: 404-778-4239

Journal of Neurotrauma
Transcriptional Changes in the Mouse Retina Following Ocular Blast Injury: A Role for the Immune System (DOI: 10.1089/neu.2017.5104)
This paper has been peer-reviewed and accepted for publication, but has yet to undergo copyediting and proof correction. The final published version may differ from this proof.

Journal of Neurotrauma
Transcriptional Changes in the Mouse Retina Following Ocular Blast Injury: A Role for the Immune System (DOI: 10.1089/neu.2017.5104)
This paper has been peer-reviewed and accepted for publication, but has yet to undergo copyediting and proof correction. The final published version may differ from this proof.

Abstract

Ocular blast injury is a major medical concern for soldiers and explosion victims due to poor visual outcomes. To define the changes in gene expression following a blast injury to the eye, we examined retinal RNA expression in 54 mouse strains five days after a single 50psi overpressure air wave blast injury. We observe that almost 40% of genes are differentially expressed with a false discovery rate of <0.001, even though the nominal changes in RNA expression are rather small. Moreover, we find through machine learning approaches that genetic networks related to the innate and acquired immune system are activated. Accompanied by lymphocyte invasion into the inner retina, blast injury also results in progressive loss of visual function and retinal ganglion cells. Collectively, these data demonstrate how systems genetics can be used to put meaning to the transcriptome changes following ocular blast injury that eventually lead to blindness.

Keywords: Ocular Blast Injury, Transcriptome, Systems Genetics, Axon Injury, Ocular Immune System

Journal of Neurotrauma
Transcriptional Changes in the Mouse Retina Following Ocular Blast Injury: A Role for the Immune System (DOI: 10.1089/neu.2017.5104)
This paper has been peer-reviewed and accepted for publication, but has yet to undergo copyediting and proof correction. The final published version may differ from this proof.

Introduction

Since the introduction of improvised explosive devices into modern warfare, the incidence rate of ocular trauma has increased dramatically from 0.65% of all battle injuries to about 13%.[1] Based on severity, these can be subdivided into penetrating or open-globe and closed-globe injuries. While open globe injuries usually require immediate medical attention, closed-globe injuries can go unnoticed. However, the latter can also lead to decreased vision.[2] For example, boxers, who frequently sustain blunt trauma to the eye, report decreasing visual function in almost half of the cases.[3] Similarly, patients suffering from Paintball ocular injuries show a visual acuity less than 20/200 in almost 60% of all reported cases.[4] The decline in vision is gradual and might not be apparent at initial examination. Recent experimental data suggest subtle axonal damage underlying the deleterious short- and long-term effects of ocular blast trauma in rodents.[5-7] The short-term (hours to days) effects include diminished pupillary reflex to red and blue light, increased cell death pathway markers and reactive gliosis. Visual function declines after a month post-blast, accompanied by gradual thinning of the nerve fiber layer and chronic pattern ERG deficits.[5] Exposure to one single blast wave is sufficient to lead to decreased axon density and glial scarring in the optic nerve observable as late as 10 months after injury, indicating that the late-onset decline in visual function is partly due to degeneration of optic nerve axons and retinal ganglion cell damage.[6] These rodent data are consistent with a report on visual dysfunction in veterans, which was strongly associated with blast injury one year after injury.[8] Thus, there seems to be a subacute phase during which retinal ganglion cells slowly degenerate, paving the way for gradual vision loss. Despite these findings, no study has systematically investigated the transcriptional changes during this sensitive time.

The present study was designed to define the influence of closed-globe blast injury on the retinal transcriptome. We examined gene expression in 52 BXD recombinant inbred (RI) mouse strains and their parental strains C57BL/6J and DBA/2J five days after exposure to a single 50psi blast wave directed to the eye. Microarray analysis was carried out at both gene and exon level, while the use of RI strains allowed for the discovery of gene regulatory networks by linking DNA sequence variants to corresponding differences in gene expression. The result is a system-wide map of gene interactions that take place 5 days after blast injury. Comparing this data to a naïve control group reveals several co-expression modules, among which we find an unexpected crosstalk of innate

Journal of Neurotrauma
Transcriptional Changes in the Mouse Retina Following Ocular Blast Injury: A Role for the Immune System (DOI: 10.1089/neu.2017.5104)
This paper has been peer-reviewed and accepted for publication, but has yet to undergo copyediting and proof correction. The final published version may differ from this proof.

and acquired immune systems. Even though the nominal changes in mRNA expression are subtle, the mutual correlation of immune system-related genes increases, in some cases drastically, suggesting activation of genetic networks.

Materials and Methods

Animals: Strains, Sex and Age

The DoD Retina Blast (Mar16) dataset contains the data of 213 Affymetrix® Mouse Gene 2.0 ST microarrays. With a total of 52 BXD strains and 2 parental strains (C57BL/6J and DBA/2J), this dataset is genotypically identical to our previously published DoD Normal Retina (May15) dataset and allows for strain-to-strain comparison. Almost all strains are represented by 4 independent biological samples usually comprising retinas from 2 male and 2 female mice between 66 and 114 days of age with a median of 76 days (Supplementary Figure 2). Animals were maintained on a 12h light – 12h dark cycle in a parasite-free facility with food and water *ad libitum*. All procedures involving animals were approved by the Animal Care and Use Committee of Emory University, Animal Use and Care Review Office (ACURO) of the USAMRMC, and were in accordance with the ARVO Statement for the Use of Animals in Ophthalmic and Vision Research.

Ocular Blast Injury Procedure

Ocular blast injury was performed using a previously described model.[6] Briefly, animals were deeply anesthetized with 67 mg/kg Tribromoethanol and secured with tape on a semi-open plastic tube sleigh. The head was safely positioned between Styrofoam nuggets to minimize blast exposure to the brain. The sleigh was then inserted into a hollow plastic cylinder with the right eye of the mouse directly facing a 7mm wide hole which was then placed in front of a custom short airgun barrel. Before every blast procedure, the output pressure was checked at the position of the eye with a pressure sensor (Honeywell, Morris Plains, NJ) and re-calibrated, if necessary, to an output of 49±1 psi (Supplementary Figure 2). The pressure sensor was fixed in place and placed flush against the tube opening. Because the thickness of the outer and inner tube (~6mm), it was not possible to position the eye closer towards the tip of the barrel than 6 mm as this would have resulted in inappropriate pressure on the eye due to squeezing it out of its orbit. Thus, there was an approx. 6mm difference in distance of the pressure transducer and the eye to the gun barrel tip.

Journal of Neurotrauma
Transcriptional Changes in the Mouse Retina Following Ocular Blast Injury: A Role for the Immune System (DOI: 10.1089/neu.2017.5104)
This paper has been peer-reviewed and accepted for publication, but has yet to undergo copyediting and proof correction. The final published version may differ from this proof.

Following a single blast, eyes were carefully investigated for signs of macroscopic damage. Eyes were lubricated with GenTeal® and mice were allowed to wake up on a heating pad. There was an overall mortality rate of 5% associated with the blast procedure. Of the 240 mice in the blast experiment, 10 died under anesthesia or during recovery. After recovery from anesthesia, 2 mice died the following day.

Functional Assessment and *Thy1*-CFP Flat Mounts

Thy1-CFP mice (n=4-7 per group) bred on a C57BL/6 background were subjected to blast and their eyes were fixed in Z-FIX (Anatech LTD, Battlecreek, MI), and washed 3 times in PBS. Retinas were dissected, mounted on slides with rails in Vectashield Hardset (Vector Laboratories, Burlingame, CA), and coverslipped.

***Thy1*-CFP Fluorescence, RGC Counting and Soma Size Assessment**

Total fluorescence of *Thy1*-CFP flat mounts was measured by quantifying green channel intensity using Photoshop CS5 without applying any further image enhancements (control n=3; blast n=4). RGC soma size was automatically measured in square pixels using a custom script in CellProfiler in 2 single frames (outer and inner) per retinal quadrant each, resulting in ~2000-

4000 RGCs identified per animal.[9] RGCs were counted using flat mounted retinas from *Thy1*-CFP mice. Briefly, each flat mount was divided into 8 regions, such that regions 1 through 4 were close to the optic nerve head (ONH) and regions 5 through 8 were towards the periphery of each flat mount. Each region consisted of a "cutbox" which was 636.5µm x 636.5µm in dimension and was prepared in Adobe Photoshop. Representative regions for each flat mount were selected and the number of CFP-positive RGC bodies were counted manually using the count tool in Photoshop. Data was averaged per group (blast, control) and determined to be significant if $p<0.05$ (Welch's t-test).

Optokinetic Tracking

Contrast sensitivity and visual acuity thresholds were measured by optokinetic tracking (OptoMotry: CerebralMechanics. Inc., Lethbridge, Alberta).[10] Briefly, the mouse was placed on a

Journal of Neurotrauma
Transcriptional Changes in the Mouse Retina Following Ocular Blast Injury: A Role for the Immune System (DOI: 10.1089/neu.2017.5104)
This paper has been peer-reviewed and accepted for publication, but has yet to undergo copyediting and proof correction. The final published version may differ from this proof.

central elevated platform in the optometry chamber surrounded by 4 monitors projecting a virtual rotating cylinder with sinusoidal gratings of vertical light and dark bars. A video camera mounted on the top of the chamber tracked the behavior of the mouse, which followed the moving gratings by turning its head, allowing to determine spatial frequency ("acuity") and contrast thresholds. Contrast sensitivity function data is expressed as the inverse of the contrast thresholds.

Sample Processing, RNA Isolation and Microarray Hybridization

Five days after the blast procedure, mice were given an overdose of Tribromoethanol and sacrificed by rapid cervical dislocation. Retinas were then dissected from eyes and directly placed into 160U/ml Ribolock® (Thermo Scientific, Walton, MA) in Hank's Balanced Salt Solution (Sigma, St. Louis, MO) on ice. Tissue was immediatel stored at -80°C. RNA was isolated using a Qiacube® and the RNeasy Mini Kit (Qiagen, Hilden, Germany) according to the manufacturer's instructions. The isolation included on-column DNase1 treatment to remove contaminating genomic DNA. All tissue was harvested between 10am and noon to minimize circadian differences in gene expression. RNA integrity was assessed on a Bioanalyzer 2100 (Agilent, Santa Clara, CA) and RIN values for all animals ranged from 8.3 to 10 with a median of 9.5 (Supplementary Figure 2). Each retina was hybridized to a separate GeneChip® Mouse Gene 2.0 ST (Affymetrix, Santa Clara, CA) according to the manufacturer's protocol. Microarray hybridization was performed by two different core laboratories: The Molecular Resource Center of Excellence at the University of Tennessee (Dr. William Taylor, Director) and the Emory Integrated Genomics Core (Dr. Michael E. Zwick, Director, and Robert B. Isett, Technical Director). In a separate experiment, we tested a set of arrays from C57BL/6J retinas at each facility to determine if there were batch effects or other confounding differences between core laboratories, but were not able to detect any. Therefore, data from both facilities were included in the analysis.

Quantitative PCR

For validation of microarray expression data, genes were randomly chosen from 4 BXD strains in both blast and normal situations. Exon-specific primers were designed using NCBI PrimerBlast and verified to be specific to the target by melting curve and gel analysis. Amplification efficiency for all primers was >90%. Primer sequences are given in Supplementary Figure 1. First strand synthesis was carried out at 42°C. using Quantitect Reverse Transcription Kit (Qiagen) and a mix of oligo(d)T

Journal of Neurotrauma
Transcriptional Changes in the Mouse Retina Following Ocular Blast Injury: A Role for the Immune System (DOI: 10.1089/neu.2017.5104)
This paper has been peer-reviewed and accepted for publication, but has yet to undergo copyediting and proof correction. The final published version may differ from this proof.

primer and random hexamers. 350µg of total RNA were retrotranscribed after incubation in gDNA eraser for 5 minutes and diluted ten-fold with ultra-pure H2O. Quantitative PCR was carried out in 10µL reactions using QuantiTect SYBR Green Master Mix (Qiagen) according to the manufacturer's instructions on a Mastercycler realplex2 (Eppendorf, Hamburg, Germany) with annealing temperature set to 60°C. Technical triplicates were averaged and normalized against *Ppia*, which was identified to be a stably expressed housekeeping gene in the retina with the help of all retinal databases found on GeneNetwork. Fold-changes were calculated in $\log_2$ using the ddCt method and compared to the microarray results by linear regression models.

Data Processing, Statistical Analysis and WGCNA

Microarray data were normalized using the Robust Multiarray Average (RMA) method[11]. Expression levels were $\log_2$-transformed, z-scored and multiplied by a factor of two before a constant of 8 was added to avoid negative expression values and make the data comparable on GeneNetwork (see GeneNetwork extended methods). Data from probes with a mean expression level lower than the 5th percentile and probes whose sequence did not have a unique BLAT hit were filtered out. Differential expression was assessed by pairwise comparison of expression values across all strains[12]. P-values were adjusted for multiple comparisons using the False Discovery Rate and a stringent cutoff of 0.001 was used to decide on statistical significance. The following parameters were chosen for weighted gene co-expression network analysis (WGCNA): A thresholding soft power of 7, for which both networks approached approximate scale-free topology. Signed topological overlap matrices were created separately and scaled appropriately to make them comparable. Modules were assigned by applying adaptive branch pruning to hierarchical clustering dendrograms with the deepSplit parameter set to 2, a minimum module size of 100, and the cutHeight set at 0.995. All analyses were performed in the R 3.1.1 statistical programming environment. The ggplot2 package for the R environment was used for most plots.[13]

Gene Enrichment Analyses and Network Graphs

Gene Ontology and KEGG pathway enrichment were assessed by submitting Affymetrix Probe IDs to WebGestalt.org.[14] Reported p-values were adjusted for multiple comparisons using Benjamini-Hochberg's FDR. Network graphs were created with Cytoscape version 3.4.

Journal of Neurotrauma
Transcriptional Changes in the Mouse Retina Following Ocular Blast Injury: A Role for the Immune System (DOI: 10.1089/neu.2017.5104)
This paper has been peer-reviewed and accepted for publication, but has yet to undergo copyediting and proof correction. The final published version may differ from this proof.

Immunostaining, Microscopy and Lymphocyte Quantification

For staining retinal flat mounts, C57BL/6J (n=4-5 per time point) mice were deeply anesthetized with Tribromoethanol and perfused through the heart with 0.9% saline followed by 4% paraformaldehyde in phosphate buffer (pH 7.4). The retinas were dissected from the globe and washed three times in phosphate buffered saline with 1% Triton X-100 (Sigma) added. Tissue was then blocked in 5% BSA (Sigma) with 0.5% Triton X-100 for one hour at room temperature. The retinas were then transferred into directly labeled primary antibodies: CD3 (HM3420, Life Technologies, 1:1000); CD4 (ab51467, Abcam, 1:1000); CD8 (MCD0828TR, Life technologies, 1:1000). After overnight incubation at 4°C., retinas were rinsed, placed on glass slides and coverslipped. The whole mounts were examined with a Nikon Ti inverted microscope with C1 confocal scanner (Nikon Instruments, Melville, NY) at 40X to identify labeled cells. Each retina was systematically scanned in the X-Y plain and Z-stacks were taken through the entire thickness of the retina. After merging all 40X images together to one picture, lymphocytes were manually counted per whole retina.

Journal of Neurotrauma
Transcriptional Changes in the Mouse Retina Following Ocular Blast Injury: A Role for the Immune System (DOI: 10.1089/neu.2017.5104)
This paper has been peer-reviewed and accepted for publication, but has yet to undergo copyediting and proof correction. The final published version may differ from this proof.

Results

Experimental design and quality of the data

To define the changes in gene expression occurring 5 days after an over-pressure blast to the eye (Figure 1A), the blast array dataset was compared to a previously published dataset from naïve retina.[15] The changes in expression were relatively modest and ranged from -0.8 to +0.6-fold on a $\log_2$ scale. The magnitude of these changes is below the arbitrary two-fold difference accepted by many microarray studies. We made a conscious decision not to analyze our results using this arbitrary cutoff for biological relevance. Instead, we controlled for statistical outliers by setting a 100-fold more stringent False Discovery Rate (FDR) than is usual for these kinds of micorarray studies.[16] We found that 13,971 genes were differentially expressed (Fig. 1B and Fig. 1C) with FDR <0.001. A subset of randomly chosen genes was used to validate the microarray results by quantitative PCR (Pearson *r* with microarray data = 0.90, Supplementary Figure 1). We were able to detect these moderate changes due to the size of both datasets and the quality of RNA samples. The blast injury dataset (DoD Retina After **Blast** Affy MoGene 2.0 ST (Mar 16), **"Blast"**) contained 213 independent biological samples from 52 BXD strains plus the two parental strains. For these microarrays, care was taken to produce high quality RNA. The average RNA integrity (RIN) score was 9.5 (±0.03, SEM) (Supplementary Figure 2). The normal retina dataset (DoD Retina Normal Affy MoGene 2.0 ST (May 15), "**Normal"**) contained a total of 222 microarrays from 55 strains and had an average RIN score of 9.4 (±0.03, SEM). An optimized RNA isolation protocol combined with the repeatability of tissue dissection results in consistency between each of the biological samples. Tissue surrounding the retina was easily excluded from the sample including the optic nerve, minimizing between-sample variation and contamination by extraneous tissues. Thus, the large number of microarrays in each data set, the quality of the RNA used to generate the data, and the consistency of tissue isolation allow our group to identify changes in gene expression with a high degree of statistical confidence. These changes may not have been seen in a smaller-sized traditional microarray or RNA-sequencing studies. Finally, both data sets are hosted on GeneNetwork.[17]

Journal of Neurotrauma
Transcriptional Changes in the Mouse Retina Following Ocular Blast Injury: A Role for the Immune System (DOI: 10.1089/neu.2017.5104)
This paper has been peer-reviewed and accepted for publication, but has yet to undergo copyediting and proof correction. The final published version may differ from this proof.

Blast injury affects the expression of distinct molecular pathways

The initial approach to the data was designed to identify differentially expressed genes and then perform functional analysis using gene enrichment profiling. Gene Ontology (GO) and Kyoto Encyclopedia of Genes and Genomes (KEGG) analysis were used to identify pathways associated with the changes observed following blast injury.[18, 19] For the down-regulated transcripts, we found significant enrichment of genes related to protein turnover and metabolic function. The largest number of significantly downregulated genes was associated with the GO term "Mitochondrion" (Fig. 2A, left panel), while for KEGG pathways, the biggest change fell in the "metabolic pathways" category (Fig 2A, right panel). Many genes encoding mitochondrial ribosomes (*Mrp**) were found within this cluster. The second largest change in GO enrichment was for the term "ATP binding" (see Supplementary Files 1 and 2 for the full list). The extent of the down-regulation of genes associated with metabolic activity reflect a clear depression of metabolic capacity within the retina as a result of blast injury. The remaining categories for down-regulated genes were primarily related to post-transcriptional molecular processes. For example, enrichment in GO terms such as "Translation" or KEGG pathways such as "Ribosome", "RNA transport" or "tRNA biosynthesis" collectively indicate protein synthesis dysregulation. Thus, at 5 days after blast injury, there is an overall decrease in genes regulating metabolic processes and genes associated with the production of finished protein products.

When we examined the genes that were up-regulated following blast injury, a very different picture emerged. Most importantly and in contrast to down-regulated genes, GO analysis was enriched in genes related to pre-transcriptional processes, such as transcriptional regulation (Fig. 2B, left panel). Additionally, up-regulated genes were specific for diverse KEGG pathways, a good half of which were related to immune system processes (Fig. 2B, right panel). For example, the pathway "Cytokine-cytokine interaction" contained many cytokines from the CC and CXL subfamily as well as the TGF-beta family. Additionally, Interferons alpha, beta, epsilon and gamma were found up-regulated within this category. These data point to a difference in transcriptional regulation as well as an increase in expression of immune response genes following blast injury, suggesting activation of the immune system similar to what our group had previously described following optic nerve crush.[20]

Journal of Neurotrauma
Transcriptional Changes in the Mouse Retina Following Ocular Blast Injury: A Role for the Immune System (DOI: 10.1089/neu.2017.5104)
This paper has been peer-reviewed and accepted for publication, but has yet to undergo copyediting and proof correction. The final published version may differ from this proof.

Network analysis of expression changes after blast injury

Gene enrichment profiling of significantly differentially expressed genes detected changes in several metabolic processes and revealed a role for the immune system following blast injury. While it is known that isolated traumatic brain injury in rodents and humans results in activation of an inflammatory cascade we wondered if these transcriptional changes would be recapitulated in the mouse retina as well.[21] Because simply looking at gene expression changes between two conditions does not reveal any information about the inherently dynamic nature of gene networks, we expanded our analysis by using unbiased machine learning algorithms that compared gene co-expression patterns across the BXD strain set.

First, we performed hierarchical clustering of expression data using weighted gene co-expression network analysis, which partitioned our data into 25 modules. These modules can be thought of as functionally different compartments of the retinal transcriptome, forming groups of highly interconnected transcripts that may shape a pathway. [22, 23] In general, there was very good preservation of modules between conditions (aggregate eigengene correlation = 0.86, see also Supplementary Figure 3), suggesting that the general gene network architecture in the retina is well conserved after blast injury and the changes seen are due to dysregulation of a small number of genes only. Genes in each module were collected and subjected to GO profiling in order to reveal the module's closest functional annotation. Among the modules with the largest drop in preservation (or the biggest changes between conditions) were three modules whose top GO terms were significantly enriched in immune system and metabolic processes, mirroring the gene enrichment profiling results (the black, blue and dark green module, Supplemental Figure 3D). We then performed GO analysis separately for up- and down-regulated genes in these three modules. This revealed a strong overrepresentation for the terms "T-cell activation" (adj. p = 0.003), "Cytokine signaling" (adj. p = 0.02) and "regulation of gene expression" (adj. p<1e-8) for up-regulated genes, while down-regulated ones were enriched for "primary metabolic process" (adj. p <1e-4) and "cellular protein metabolic process" (adj. p = 0.004).

Another way to examine gene network differences between conditions would be to look at changes of gene connectivity. This measure assigns an arbitrary number to a gene that represents how well its expression correlates to other genes.[24] Changes in connectivity mirror the dynamic nature of gene regulatory networks; an increase can be thought of as activation of a gene network and vice versa.[25] We performed gene ontology analysis for the top percentile of genes with changes in connectivity. GO trees were very detailed, with genes having the highest increase in

Journal of Neurotrauma
Transcriptional Changes in the Mouse Retina Following Ocular Blast Injury: A Role for the Immune System (DOI: 10.1089/neu.2017.5104)
This paper has been peer-reviewed and accepted for publication, but has yet to undergo copyediting and proof correction. The final published version may differ from this proof.

connectivity enriched in the terms “cell adhesion” (adj. p=0.025), “macrophage apoptotic process” (adj. p = 0.019), “extracellular region” (adj. p = 0.014), “regulation of immunoglobulin-mediated immune response” (adj. p < 0.001), as well as “isotype switching to IgG subtypes” (adj. p < 0.001). On the other hand, genes whose connectivity dropped were associated with the GO terms “axonogenesis”, “synaptic transmission”, “dendrite” (all adj. p <1e-8), “synapse” (adj. p < 1e-12), “protein kinase activity”, and “ATP binding” (both adj. p < 0.001), indicating that normal transcriptional regulation of these molecular processes or entities was impaired after blast injury.

In summary, these results suggest three dominating biologically relevant processes as a result of ocular blast injury: Loss of synaptic transmission, impaired cell metabolism as well as activation of the immune system.

Activation of innate and acquired immune system

Our analysis of the effects of blast injury on gene expression defined a series of differentially expressed genes and many of these genes clustered into GO categories and KEGG pathways associated with the innate immune system. Earlier work from our group has revealed an activation of the innate immune network following optic nerve crush (ONC).[20] Since ONC is a well-studied model of retinal ganglion cell damage, we wondered whether or not we would find activation of immune system-related gene networks in the blast data as well. When we examined the blast injury dataset, we saw higher expression levels for many of the same genes (Table I). Even though some of these genes did not reach significance regarding their differential expression, there was a dramatic increase in mutual correlations to genes involved in innate immunity processes (Fig. 3A). This suggested that the system is indeed activated. When we expanded this analysis for the top 200 correlates of *C4b* (a gene essential for the propagation of the classic complement cascade), we observed a strikingly strong mutual correlation in the blast but not in the normal condition (Fig. 3B). Gene Ontology terms for these top 200 correlates of C4b revealed highly significant involvement in multiple immune system-related biological processes and pathways (Fig. 3C), confirming the involvement of the innate immune system.

This acute activation also coincided with an increase in markers of the acquired immune system. There was a significant (adj. p < 0.001) increase in the gene expression levels of *Cd3* and *Cd8* (known markers of T-lymphocytes) in our microarray datasets. Others have shown infiltration of T-cells into the CNS and retina under pathological conditions.[26, 27] To determine if this was also

Journal of Neurotrauma
Transcriptional Changes in the Mouse Retina Following Ocular Blast Injury: A Role for the Immune System (DOI: 10.1089/neu.2017.5104)
This paper has been peer-reviewed and accepted for publication, but has yet to undergo copyediting and proof correction. The final published version may differ from this proof.

the case after blast, we examined the retina at 7, 14 and 28 days following blast injury. At 7 days, CD3-positive cells were observed invading the retina and most of these cells were found in the inner nuclear layer, in close proximity to the intraretinal vessels (Fig. 4A) and this increase was significant ($p<0.0001$). At 14 days, there was an increase in the number of CD3/CD4 double-positive lymphocytes (T-helper cells). By 28 days after blast, many CD3-positive cells remained within the retina and in addition to the presence of CD3/CD4-positive T-helper cells, a few CD3/CD8 cytotoxic T-cells were observed (Fig. 4B). Our results are consistent with other research investigating lymphocyte invasion into the retina. For example, it was shown in a model of autoimmune uveitis that CD4+ T-cells predominate during the early phase, while CD8+ T-cells accumulate in later stages.[28] The identification of T-cells in the injured retina supports the view that cellular immune mechanisms could be responsible for the tissue damage caused by blast injury.

One potential link between the activation of the innate immune system and the infiltration of lymphocytes could be through a series of soluble factors such as pro-inflammatory cytokines *Cxcr3*, *Ccl4* and IFN-gamma, all of which are expressed in the injured retina.[29-31] These cytokines and chemokines, which are released after injury by glial or endothelial cells, may play crucial roles in the recruitment of T-lymphocytes to the injured retina. Even though of these three cytokines only IFN-gamma was significantly upregulated after blast (adj. p=2.5 e-06), this hypothesis is at least partially supported by increased correlations of all three cytokines to *Cd3* in our blast database (Fig 4C).

Ocular blast injury leads to progressive vision loss associated with loss of retinal ganglion cells

The transcriptional changes observed at 5 days following a blast injury represent a small series of molecular cascades that may result in progressive loss of visual function and the death of retinal ganglion cells (RGCs). Because the functional changes that eventually lead to blindness may not be apparent as early as 5 days after blast, we assayed RGC features and function at different time points.

Many genes can serve as proxy for the identification of RGCs[32], and when we investigated our data for changes in these markers, we surprisingly observed higher expression of many of these after blast (***Thy1, Tubb3, Pou4f2***, *Pou4f1, Rbpms*, bold ones are significant at $p<0.001$). For example, the generic RGC marker *Thy1* showed a 0.2-fold $\log_2$ change (adj. p = 2.16e-6). We confirmed this upregulation by measuring the total fluorescence of flat-mounted retinas from

Thy1-CFP transgenic animals at 1 week (Fig. 5A). At the same time point, we also observed a significant increase in RGC soma size (Fig. 5B). Both total fluorescence and RGC soma size were significantly decreased at 6 weeks after blast. Functional measures at 6 weeks were also diminished in the same mice, as evidenced by a moderate drop in visual acuity and a dramatic drop in contrast sensitivity (Fig. 5C). Along with that, we observed a ~16% loss of *Thy1*-CFP-positive RGCs, ultimately identifying the culprit of ongoing vision loss (Fig. 5D). Taken together, these data demonstrate the devastating effects of what appears to be a relatively modest injury. They also reinforce the importance for early treatment, as the transcriptional events that are observable as early as 5 days after blast eventually lead to blindness.

Journal of Neurotrauma
Transcriptional Changes in the Mouse Retina Following Ocular Blast Injury: A Role for the Immune System (DOI: 10.1089/neu.2017.5104)
This paper has been peer-reviewed and accepted for publication, but has yet to undergo copyediting and proof correction. The final published version may differ from this proof.

Journal of Neurotrauma
Transcriptional Changes in the Mouse Retina Following Ocular Blast Injury: A Role for the Immune System (DOI: 10.1089/neu.2017.5104)
This paper has been peer-reviewed and accepted for publication, but has yet to undergo copyediting and proof correction. The final published version may differ from this proof.

Discussion

This study comprehensively characterized the in vivo effects of blast injury to the mouse retina and offers the first report on the systems genetics of ocular blast injury. A few other studies have previously investigated the molecular effects of ocular blast injury, and we note that the pressures used to inflict injury differ between models. While one study reported globe rupture at pressures of 40psi and more, this was not the case in our model.[6] In preliminary experiments using our gun, we did not see globe ruptures until pressures more than 70psi were reached. One possible explanation for this difference could be variation in build of the models or placement of the pressure transducer (see Methods). It is likely that the effective pressure reaching the back of the eye is closer to the range previously reported (<30psi), as there was an approximate 6mm distance between the tip of the barrel and the eye. Nevertheless, calibration to 50psi at the tip of the barrel was necessary to avoid technical variance in the blast apparatus. This pressure is comparable to the amount of pressure sustained at the epicenter of a grenade explosion, making this model roughly equivalent to being a few steps away from a grenade or bomb explosion (as pressure decreases with the cube of distance).[33] Here, we presented evidence that a single 50psi ocular blast as measured at the tip of the airgun barrel was sufficient to lead to declining visual function. This progression was accompanied by a steady increase in the number of lymphocytes migrating into the retina (Figure 6).

While it is currently unknown whether this confers a regenerative or destructive effect, in many ways the pathology of ocular blast injury appears to be closely related to traumatic brain injury (TBI). It is believed that in TBI, early-phase leukocyte-mediated breakdown of the blood-brain-barrier eventually leads to vascular and synapse remodeling.[34] The ensuing neurodegeneration manifests itself as depression or anxiety in TBI or, in the case of ocular blast, as blindness. In mice, the negative neurological outcomes seen in TBI can be mitigated through inhibition of lymphocyte-mediated signaling, while the decline in visual function after ocular blast injury can be reduced through immediate-early administration of NSAIDs like Meloxicam (P. Michael Iuvone, unpublished data).[35, 36] Since this inflammatory response seems to occur in an acute and chronic phase over an extended period of time, treatment strategies have a wide therapeutic window. Early immunomodulatory treatments in the acute or subacute phase could have dramatic effects on the chronic response. Thus, it is appropriate to investigate the transcriptional changes at the transition from an acute to a chronic state, as the invasion of lymphocytes into the retina likely marks an irreversibly damaging process.

Journal of Neurotrauma
Transcriptional Changes in the Mouse Retina Following Ocular Blast Injury: A Role for the Immune System (DOI: 10.1089/neu.2017.5104)
This paper has been peer-reviewed and accepted for publication, but has yet to undergo copyediting and proof correction. The final published version may differ from this proof.

Towards that end, we monitored the retinal transcriptome 5 days after blast injury, and found that a vast number of genes was differentially expressed at that time despite none of the changes exceeding two-fold. A potential reason for this is the fact that we analyzed whole retina, which contains >7 cell types, but our and others' results indicate that the pathological changes mostly occur in fewer cell types (RGCs and glial cells), which together make up less than 1% of cells in the retina.[37] As such, most of the RNA that microarrays were normalized to is contributed by the likely unaffected photoreceptors, the most abundant cell type in the retina. Thus, even though it could be very possible that larger fold-changes exist in the affected cell populations, they are not seen in the whole retina data. Instead of focusing on a biologically relevant cutoff, we therefore strongly controlled for statistical outliers by setting a stringent FDR. Our results indicate that transcriptional changes originating from extracellular signaling pathways are dominating the ocular environment five days after blast, which comes at the expense of the cells' metabolic function, RNA processing and protein production. It is not surprising that the largest number of downregulated genes after blast injury was associated with mitochondria, as dysregulated mitochondrial metabolism has long been known to play a significant role in TBI.[38] While actual uncoupling of ATP synthesis from the respiratory chain would result in mitochondrial stress and acute cell death, other more low-grade mechanisms of mitochondrial dysfunction must be responsible for the slow neurodegeneration that manifests itself after blast injury in the retina. It has very recently been shown that mitochondrial fission is strongly increased in TBI, and that the negative effects on learning and memory could be rescued through the administration of a fission inhibitor.[39] It would be interesting to investigate if similar improvements of metabolic function could be achieved in ocular blast injury.

Other changes in gene expression we observed between blasted and normal mice were seemingly related to the balance between transcription and translation. Along with a decrease in genes responsible for ribosomal or endoplasmic reticulum function, we found increased expression of many transcription factors and cofactors. This mirrors the dynamic nature of gene regulatory networks. Changes in RNA expression measured in total tissue are either due to one specific cell type adapting its transcriptional program to a stimulus, or additional new cells that became part of the whole cell population. While it is likely that a small fraction of the changes seen is the result of lymphocyte invasion, a large part of the differentially expressed RNA will be contributed from retinal cells synthesizing regulatory molecules that prepare the cell for the changes to come.

Because ocular blast injury was previously associated with thinning of the retinal nerve fiber layer we investigated RGC function as well as expression changes in RGC marker genes.[7]

Journal of Neurotrauma
Transcriptional Changes in the Mouse Retina Following Ocular Blast Injury: A Role for the Immune System (DOI: 10.1089/neu.2017.5104)
This paper has been peer-reviewed and accepted for publication, but has yet to undergo copyediting and proof correction. The final published version may differ from this proof.

Interestingly, we saw statistically significant increased expression in genes such as *Thy1*, which also corresponded to an increase in RGC soma size and *Thy1*-CFP fluorescence. This could be related to a process termed neuronal chromatolysis, a cellular response after axonal damage resulting in the dissolution of Nissl bodies and redistribution of cytoskeletal proteins with an apparent increase in soma size.[40] As chromatolytic neurons are thought to still possess the ability to regenerate, it is interesting to speculate whether or not treatment at this time would stall neuronal apoptosis. We and others have observed that the decline in retinal ganglion cell number or nerve fiber layer thickness is gradual, suggesting a slow but constant underlying molecular process. It appears that this process is related to immune signaling, as our enrichment analysis identified the strongest positive change in expression in genes related to the immune system. Even when the changes in mRNA levels were not significant, increased correlation and connectivity of co-expressed genes was seen especially for immunity-related genes. This illustrates activation of genetic networks, which we have previously found to be the case in the same mouse population after optic nerve crush.[20] In ONC, a fixed amount of pressure is applied to the optic nerve without interrupting the blood flow to the retina, which leads to gradual decline in retinal ganglion cell number.[41] Therefore, both ONC and blast injury are models for RGC death, in which the immune signaling cascade appears to play a significant role. The exact molecular cascades leading to this have yet to be determined, but it is likely that cytokine signaling plays a significant role. Other studies suggest that expression of cytokines in the retina is mediated by glial cells and that an increase in cytokine signaling results in activation of retinal microglia, astrocytes and Müller glia on site.[42, 43] In our analysis, we saw that *C4b* formed a genetic network after blast injury that was significantly enriched in the cellular GO terms “Macrophages” and “Microglia”. The parent protein of *C4b* is complement factor C4. It is now known for about 20 years that microglia and astrocytes in mouse brains can synthesize complement factors[44] and it was also shown that complement genes are expressed in the retina.[45] While the exact origin of complement factor secretion in the retina remains unknown, our and others’ results indicate a role for microglia in this process. It is interesting to note that *C4b* correlates were also enriched for the terms “Epithelium”, “Extracellular Matrix” and “Integrin Binding”. This could suggest that one of the of the mechanisms that permit lymphocyte invasion through the otherwise tight blood-retina barrier after blast is mediated through breakdown of the blood-retina barrier by molecules secreted from microglia activated by complement factors. Similar processes have been observed in TBI as well.[46, 47]

Ultimately, the DBA/2J mouse is known for having several immune system-related defects compared to the C57BL/6J mouse.[48, 49] Among these is a condition that abrogates ocular immune

Journal of Neurotrauma
Transcriptional Changes in the Mouse Retina Following Ocular Blast Injury: A Role for the Immune System (DOI: 10.1089/neu.2017.5104)
This paper has been peer-reviewed and accepted for publication, but has yet to undergo copyediting and proof correction. The final published version may differ from this proof.

privilege associated with the anterior chamber, called a dysfunctional anterior chamber associated immune deviation (ACAID). [50] This syndrome was recently found to be at least in part due to a dysfunctional Natural Killer Cell system resulting from *Cd94* deficiency in DBA/2J mice.[51] We examined our databases for correlations between the presence (B6 genotype) or absence (D2 genotype) of ACAID and inflammatory markers, but no significant correlation was found (data not shown). While another study has detected greater influx of immune components into the anterior part of the eye in DBA/2J mice after blast injury, our data suggest no such connection for retina.[43] This indicates that lymphocyte infiltration into the retina is independent of a functional or dysfunctional ACAID.

In conclusion, our data reveal the genetic networks of ocular blast injury for the first time. Using a systems genetics approach, we show that the dysregulated transcriptional environment is reminiscent of the pathophysiology of TBI, with loss of metabolic function and activation of inflammatory cascades that eventually lead to decreases in visual function. Having used BXD strains for this study will potentially allow to identify upstream modulators of this immune cascade as future work. To our knowledge, this is by far the largest microarray study on ocular blast injury, and it is our hope that the publically available data will be useful for fellow researchers who are interested in specific genes or pathways involved in the pathogenesis of blast injury.

Acknowledgements: This study was supported by the DoD CDMRP Grant W81XWH1210255 and W81XWH-12-1-0436 from the USA Army Medical Research & Material Command and the Telemedicine and Advanced Technology (EEG, PMI), NEI grants R01EY178841 (EEG) R01EY004864 (PMI), P30EY06360 (Emory Vision Core, PMI), and Unrestricted Funds from Research to Prevent Blindness. FLS is supported by the institutional training grant T32EY007092-30 (PMI). Additional support was provided by the Emory Integrated Genomics Core (EIGC), which is subsidized by the Emory University School of Medicine as one of the Emory Integrated Core Facilities. We want to thank Dr. Robert Williams and Arthur Centeno (University of Tennessee Health Science Center) for maintaining the data on GeneNetwork, Dr. Xiangdi Wang and Dr. Justin Templeton for their technical assistance as well as April Brooke Still for her help in breeding some BXD animals at Emory University.

Author Statement: The study was conceived by EEG. RK collected and isolated RNA from most of the animals. FLS performed the blast procedure and all statistical and bioinformatic analyses. YL was responsible for lymphocyte immunostaining and counting. MC compiled *Thy1*-CFP flat mounts and helped with animal breeding. CS and PL completed the OKT experiments overseen by PMI. FLS, EEG and YL wrote the paper with input from all other authors. All authors read and approved the final manuscript.

Journal of Neurotrauma
Transcriptional Changes in the Mouse Retina Following Ocular Blast Injury: A Role for the Immune System (DOI: 10.1089/neu.2017.5104)
This paper has been peer-reviewed and accepted for publication, but has yet to undergo copyediting and proof correction. The final published version may differ from this proof.

References

1. Weichel, E.D. and M.H. Colyer (2008). Combat ocular trauma and systemic injury. Curr Opin Ophthalmol 19, 519-25.

2. Cockerham, G.C., T.A. Rice, E.H. Hewes, K.P. Cockerham, S. Lemke, G. Wang, R.C. Lin, C. Glynn-Milley, and L. Zumhagen (2011). Closed-eye ocular injuries in the Iraq and Afghanistan wars. N Engl J Med 364, 2172-3.

3. Corrales, G. and A. Curreri (2009). Eye trauma in boxing. Clin Sports Med 28, 591-607, vi.

4. Nemet, A.Y., L. Asalee, Y. Lang, D. Briscoe, and E.I. Assia (2016). Ocular Paintball Injuries. Isr Med Assoc J 18, 27-31.

5. Bricker-Anthony, C., J. Hines-Beard, and T.S. Rex (2014). Molecular changes and vision loss in a mouse model of closed-globe blast trauma. Invest Ophthalmol Vis Sci 55, 4853-62.

6. Hines-Beard, J., J. Marchetta, S. Gordon, E. Chaum, E.E. Geisert, and T.S. Rex (2012). A mouse model of ocular blast injury that induces closed globe anterior and posterior pole damage. Exp Eye Res 99, 63-70.

7. Mohan, K., H. Kecova, E. Hernandez-Merino, R.H. Kardon, and M.M. Harper (2013). Retinal ganglion cell damage in an experimental rodent model of blast-mediated traumatic brain injury. Invest Ophthalmol Vis Sci 54, 3440-50.

8. Dougherty, A.L., A.J. MacGregor, P.P. Han, K.J. Heltemes, and M.R. Galarneau (2011). Visual dysfunction following blast-related traumatic brain injury from the battlefield. Brain Inj 25, 8-13.

9. Carpenter, A.E., T.R. Jones, M.R. Lamprecht, C. Clarke, I.H. Kang, O. Friman, D.A. Guertin, J.H. Chang, R.A. Lindquist, J. Moffat, P. Golland, and D.M. Sabatini (2006). CellProfiler: image analysis software for identifying and quantifying cell phenotypes. Genome Biol 7, R100.

Journal of Neurotrauma
Transcriptional Changes in the Mouse Retina Following Ocular Blast Injury: A Role for the Immune System (DOI: 10.1089/neu.2017.5104)
This paper has been peer-reviewed and accepted for publication, but has yet to undergo copyediting and proof correction. The final published version may differ from this proof.

10. Douglas, R.M., N.M. Alam, B.D. Silver, T.J. McGill, W.W. Tschetter, and G.T. Prusky (2005). Independent visual threshold measurements in the two eyes of freely moving rats and mice using a virtual-reality optokinetic system. Vis Neurosci 22, 677-84.

11. Irizarry, R.A., B. Hobbs, F. Collin, Y.D. Beazer-Barclay, K.J. Antonellis, U. Scherf, and T.P. Speed (2003). Exploration, normalization, and summaries of high density oligonucleotide array probe level data. Biostatistics 4, 249-64.

12. Cheadle, C., M.P. Vawter, W.J. Freed, and K.G. Becker (2003). Analysis of microarray data using Z score transformation. J Mol Diagn 5, 73-81.

13. Wickham, H., 2009. Ggplot2 : elegant graphics for data analysis. Use R! 2009, New York: Springer. viii, 212 p.

14. Wang, J., D. Duncan, Z. Shi, and B. Zhang (2013). WEB-based GEne SeT AnaLysis Toolkit (WebGestalt): update 2013. Nucleic Acids Res 41, W77-83.

15. King, R., L. Lu, R.W. Williams, and E.E. Geisert (2015). Transcriptome networks in the mouse retina: An exon level BXD RI database. Mol Vis 21, 1235-51.

16. Gusnanto, A., S. Calza, and Y. Pawitan (2007). Identification of differentially expressed genes and false discovery rate in microarray studies. Curr Opin Lipidol 18, 187-93.

17. Mulligan, M.K., K. Mozhui, P. Prins, and R.W. Williams (2017). GeneNetwork: A Toolbox for Systems Genetics. Methods Mol Biol 1488, 75-120.

18. Gene Ontology, C. (2015). Gene Ontology Consortium: going forward. Nucleic Acids Res 43, D1049-56.

19. Kanehisa, M., Y. Sato, M. Kawashima, M. Furumichi, and M. Tanabe (2016). KEGG as a reference resource for gene and protein annotation. Nucleic Acids Res 44, D457-62.

20. Templeton, J.P., N.E. Freeman, J.M. Nickerson, M.M. Jablonski, T.S. Rex, R.W.

Journal of Neurotrauma
Transcriptional Changes in the Mouse Retina Following Ocular Blast Injury: A Role for the Immune System (DOI: 10.1089/neu.2017.5104)
This paper has been peer-reviewed and accepted for publication, but has yet to undergo copyediting and proof correction. The final published version may differ from this proof.

Williams, and E.E. Geisert (2013). Innate immune network in the retina activated by optic nerve crush. Invest Ophthalmol Vis Sci 54, 2599-606.

21. Holmin, S., T. Mathiesen, J. Shetye, and P. Biberfeld (1995). Intracerebral inflammatory response to experimental brain contusion. Acta Neurochir (Wien) 132, 110-9.

22. Langfelder, P. and S. Horvath (2008). WGCNA: an R package for weighted correlation network analysis. BMC Bioinformatics 9, 559.

23. Fuller, T.F., A. Ghazalpour, J.E. Aten, T.A. Drake, A.J. Lusis, and S. Horvath (2007). Weighted gene coexpression network analysis strategies applied to mouse weight. Mamm Genome 18, 463-72.

24. Langfelder, P., P.S. Mischel, and S. Horvath (2013). When is hub gene selection better than standard meta-analysis? PLoS One 8, e61505.

25. Zhao, W., P. Langfelder, T. Fuller, J. Dong, A. Li, and S. Hovarth (2010). Weighted gene coexpression network analysis: state of the art. J Biopharm Stat 20, 281-300.

26. Charteris, D.G., C. Champ, A.R. Rosenthal, and S.L. Lightman (1992). Behcet's disease: activated T lymphocytes in retinal perivasculitis. Br J Ophthalmol 76, 499-501.

27. Imagawa, T., H. Kitagawa, and M. Uehara (2003). Appearance of T cell subpopulations in the chicken and embryo retina. J Vet Med Sci 65, 23-8.

28. Richardson, P.R., M.E. Boulton, J. Duvall-Young, and D. McLeod (1996). Immunocytochemical study of retinal diode laser photocoagulation in the rat. Br J Ophthalmol 80, 1092-8.

29. Ha, Y., H. Liu, Z. Xu, H. Yokota, S.P. Narayanan, T. Lemtalsi, S.B. Smith, R.W. Caldwell, R.B. Caldwell, and W. Zhang (2015). Endoplasmic reticulum stress-regulated CXCR3 pathway mediates inflammation and neuronal injury in acute glaucoma. Cell Death Dis 6, e1900.

Journal of Neurotrauma
Transcriptional Changes in the Mouse Retina Following Ocular Blast Injury: A Role for the Immune System (DOI: 10.1089/neu.2017.5104)
This paper has been peer-reviewed and accepted for publication, but has yet to undergo copyediting and proof correction. The final published version may differ from this proof.

30. Rutar, M., R. Natoli, R.X. Chia, K. Valter, and J.M. Provis (2015). Chemokine-mediated inflammation in the degenerating retina is coordinated by Muller cells, activated microglia, and retinal pigment epithelium. J Neuroinflammation 12, 8.

31. Zinkernagel, M.S., H.R. Chinnery, M.L. Ong, C. Petitjean, V. Voigt, S. McLenachan, P.G. McMenamin, G.R. Hill, J.V. Forrester, M.E. Wikstrom, and M.A. Degli-Esposti (2013). Interferon gamma-dependent migration of microglial cells in the retina after systemic cytomegalovirus infection. Am J Pathol 182, 875-85.

32. Struebing, F.L., R.K. Lee, R.W. Williams, and E.E. Geisert (2016). Genetic Networks in Mouse Retinal Ganglion Cells. Front Genet 7, 169.

33. Glasstone, S. and P. Dolan, 1977. The Effects of Nuclear Weapons. 1977: United States Department of Defense.

34. Schwarzmaier, S.M., R. Zimmermann, N.B. McGarry, R. Trabold, S.W. Kim, and N. Plesnila (2013). In vivo temporal and spatial profile of leukocyte adhesion and migration after experimental traumatic brain injury in mice. J Neuroinflammation 10, 32.

35. Wood, R.L. and N.A. Rutterford (2006). Demographic and cognitive predictors of long-term psychosocial outcome following traumatic brain injury. J Int Neuropsychol Soc 12, 350-8.

36. Zhao, S., Z. Yu, Y. Liu, Y. Bai, Y. Jiang, K. van Leyen, Y.G. Yang, J.M. Lok, M.J. Whalen, E.H. Lo, and X. Wang (2016). CD47 deficiency improves neurological outcomes of traumatic brain injury in mice. Neurosci Lett 643, 125-130.

37. Jeon, C.J., E. Strettoi, and R.H. Masland (1998). The major cell populations of the mouse retina. J Neurosci 18, 8936-46.

38. Vink, R., V.A. Head, P.J. Rogers, T.K. McIntosh, and A.I. Faden (1990). Mitochondrial metabolism following traumatic brain injury in rats. J Neurotrauma 7, 21-7.

39. Fischer, T.D., M.J. Hylin, J. Zhao, A.N. Moore, M.N. Waxham, and P.K. Dash (2016). Altered Mitochondrial Dynamics and TBI Pathophysiology. Front Syst Neurosci 10,

29.

40. Chen, D.H. (1978). Qualitative and quantitative study of synaptic displacement in chromatolyzed spinal motoneurons of the cat. J Comp Neurol 177, 635-64.

41. Templeton, J.P. and E.E. Geisert (2012). A practical approach to optic nerve crush in the mouse. Mol Vis 18, 2147-52.

42. Stahl, T., C. Mohr, J. Kacza, C. Reimers, T. Pannicke, C. Sauder, A. Reichenbach, and J. Seeger (2003). Characterization of the acute immune response in the retina of Borna disease virus infected Lewis rats. J Neuroimmunol 137, 67-78.

43. Bricker-Anthony, C., J. Hines-Beard, L. D'Surney, and T.S. Rex (2014). Exacerbation of blast-induced ocular trauma by an immune response. J Neuroinflammation 11, 192.

44. Haga, S., T. Aizawa, T. Ishii, and K. Ikeda (1996). Complement gene expression in mouse microglia and astrocytes in culture: comparisons with mouse peritoneal macrophages. Neurosci Lett 216, 191-4.

45. Luo, C., M. Chen, and H. Xu (2011). Complement gene expression and regulation in mouse retina and retinal pigment epithelium/choroid. Mol Vis 17, 1588-97.

46. Baskaya, M.K., A.M. Rao, A. Dogan, D. Donaldson, and R.J. Dempsey (1997). The biphasic opening of the blood-brain barrier in the cortex and hippocampus after traumatic brain injury in rats. Neurosci Lett 226, 33-6.

47. Balu, R. (2014). Inflammation and immune system activation after traumatic brain injury. Curr Neurol Neurosci Rep 14, 484.

48. Casanova, T., E. Van de Paar, D. Desmecht, and M.M. Garigliany (2015). Hyporeactivity of Alveolar Macrophages and Higher Respiratory Cell Permissivity Characterize DBA/2J Mice Infected by Influenza A Virus. J Interferon Cytokine Res 35, 808-20.

49. Miyairi, I., V.R. Tatireddigari, O.S. Mahdi, L.A. Rose, R.J. Belland, L. Lu, R.W. Williams, and G.I. Byrne (2007). The p47 GTPases Iigp2 and Irgb10 regulate innate immunity

Journal of Neurotrauma
Transcriptional Changes in the Mouse Retina Following Ocular Blast Injury: A Role for the Immune System (DOI: 10.1089/neu.2017.5104)
This paper has been peer-reviewed and accepted for publication, but has yet to undergo copyediting and proof correction. The final published version may differ from this proof.

and inflammation to murine Chlamydia psittaci infection. J Immunol 179, 1814-24.

50. Streilein, J.W. and J.Y. Niederkorn (1981). Induction of anterior chamber-associated immune deviation requires an intact, functional spleen. J Exp Med 153, 1058-67.

51. Chattopadhyay, S., J. O'Rourke, and R.E. Cone (2008). Implication for the CD94/NKG2A-Qa-1 system in the generation and function of ocular-induced splenic CD8+ regulatory T cells. Int Immunol 20, 509-16.

Affymetrix Probe	Symbol	Description	significant at FDR < 0.001 (blast vs. normal)	Mean Expression [log2]		Correlation: Pearson's r		p-values (Pearson)	
				Normal	Blast	Normal	Blast	Normal	Blast
17343918	*C4b*	complement component 4B	no	8.56	8.62	**1**	**1**		
17346528	*C3*	complement component 3	no	7.81	7.95	0.56	0.80	0.000007	0
17387517	*Serping1*	serine peptidase inhibitor, clade G, member 1	no	9.14	9.07	0.54	0.76	0.000014	0
17462492	*A2m*	alpha-2-macroglobulin	no	8.85	8.83	0.32	0.75	0.015840	0
17417976	*Edn2*	endothelin 2	no	8.03	8.14	0.43	0.75	0.001010	0
17212750	*Stat1*	signal transducer and activator of transcription 1	no	10.31	10.33	0.40	0.71	0.002010	0.000002
17350982	*Cd74*	CD74 antigen	no	8.45	8.51	0.27	0.65	0.046220	0.000006
17269717	*Stat3*	signal transducer and activator of transcription 3	**yes**	10.92	11.10	0.54	0.65	0.000017	0
17546109	*Tlr7*	toll-like receptor 7	no	6.36	6.32	0.09	0.63	0.379190	0.000013

17414836	*Tlr4*	toll-like receptor 4	**yes**	7.05	7.16	0.29	0.61	0.030960	0.000001
17515074	*Icam1*	intercellular adhesion molecule 1	no	8.05	8.10	0.46	0.55	0.000370	0.000006

Journal of Neurotrauma
Transcriptional Changes in the Mouse Retina Following Ocular Blast Injury: A Role for the Immune System (DOI: 10.1089/neu.2017.5104)
This paper has been peer-reviewed and accepted for publication, but has yet to undergo copyediting and proof correction. The final published version may differ from this proof.

Figure Legends

Figure 1

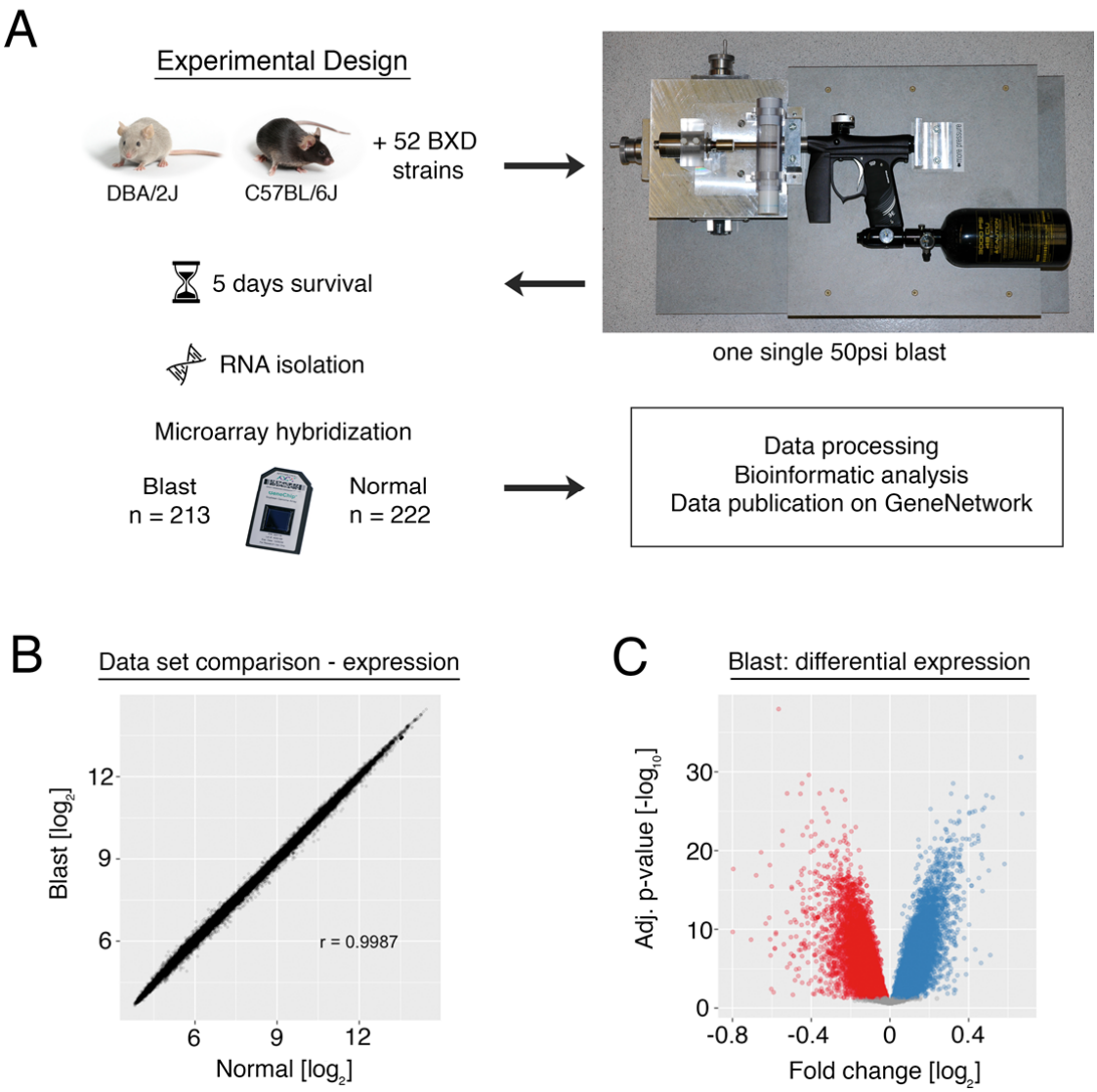

Figure 1: (A) Experimental Design. Mice were subjected to a single ocular 50psi blast wave in the apparatus depicted on the right. RNA was isolated 5 days after injury and hybridized to the Affymetrix GeneChip® Mouse Gene ST 2.0 microarray. (B) Correlation of microarray probes between the blast and the normal data set. In this scatterplot, each dot represents one unique microarray probe. The total correlation (Pearson's r) is 0.999. (C) Volcano plot showing fold-change after blast and its associated logarithmic p-value after adjustment for multiple comparisons using

an FDR of 0.001. Each dot represents one microarray probe. Red: Down-regulated probes. Blue: Up-regulated probes. Grey: No significant change at FDR<0.001.

Journal of Neurotrauma
Transcriptional Changes in the Mouse Retina Following Ocular Blast Injury: A Role for the Immune System (DOI: 10.1089/neu.2017.5104)
This paper has been peer-reviewed and accepted for publication, but has yet to undergo copyediting and proof correction. The final published version may differ from this proof.

Figure 2

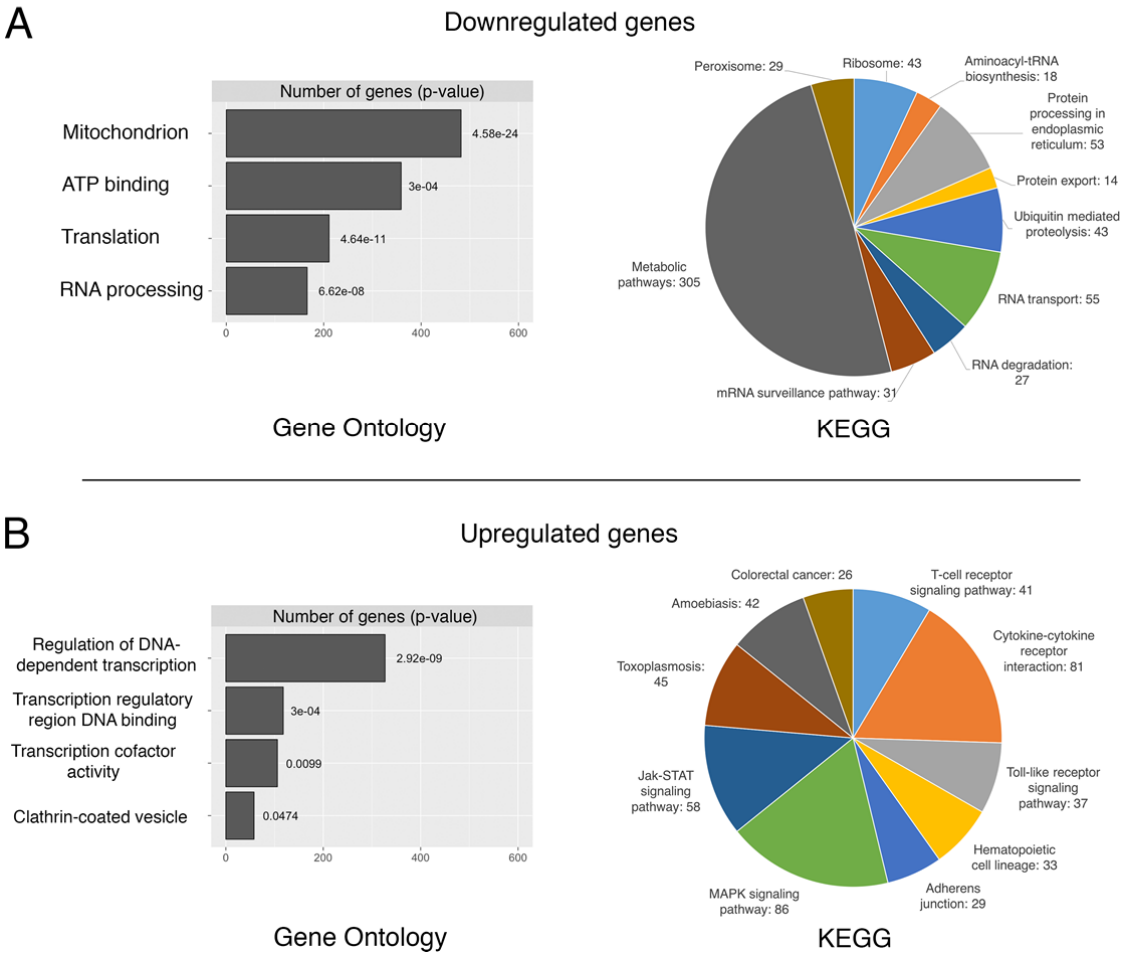

Figure 2: (A) The left-hand plot shows the number and associated adjusted p-value of significantly downregulated genes and their top 4 Gene Ontology (GO) terms. The right-hand pie chart indicates significant Kyoto Encyclopedia of Genes and Genomes (KEGG) pathway enrichment for the same genes. (B) Identical to (A), but for significantly upregulated genes after blast injury.

Journal of Neurotrauma
Transcriptional Changes in the Mouse Retina Following Ocular Blast Injury: A Role for the Immune System (DOI: 10.1089/neu.2017.5104)
This paper has been peer-reviewed and accepted for publication, but has yet to undergo copyediting and proof correction. The final published version may differ from this proof.

Figure 3

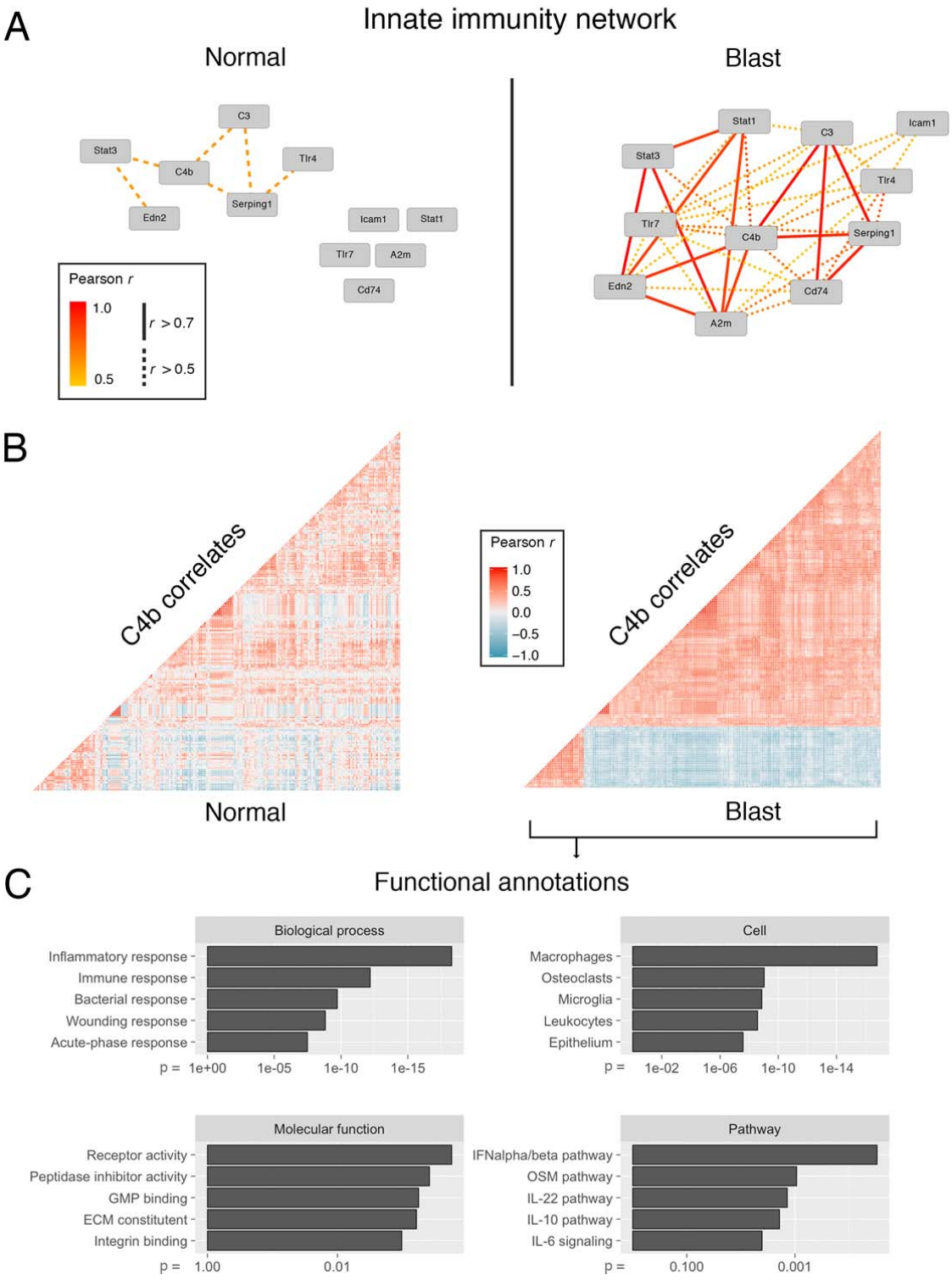

Figure 3: (A) Network graph displaying Pearson's *r* for select innate immunity genes in the normal (left) and blast injury (right) situation. While there is little correlation in the normal condition, the innate immunity network is activated after blast. (B) Correlation matrices showing mutual Pearson's *r* for the top 200 correlates of the gene *C4b*. Each dot represents one gene. Hierarchical clustering was applied to the blast matrix and genes did not change position between conditions. There is a strong increase in the mutual correlations indicating activation of a genetic network centered around *C4b* in the blast condition. (C) Top 5 Gene Ontology (GO) terms for the *C4b* correlates shown in (B). The adjusted p-value is indicated on the x-axis. GO enrichment demonstrates a strong relationship of *C4b* correlates to the immune system. GMP = Guanosine monophosphate synthetase, ECM = extracellular matrix, OSM = Oncostatin M, IL = Interleukin

Journal of Neurotrauma
Transcriptional Changes in the Mouse Retina Following Ocular Blast Injury: A Role for the Immune System (DOI: 10.1089/neu.2017.5104)
This paper has been peer-reviewed and accepted for publication, but has yet to undergo copyediting and proof correction. The final published version may differ from this proof.

Journal of Neurotrauma
Transcriptional Changes in the Mouse Retina Following Ocular Blast Injury: A Role for the Immune System (DOI: 10.1089/neu.2017.5104)
This paper has been peer-reviewed and accepted for publication, but has yet to undergo copyediting and proof correction. The final published version may differ from this proof.

Figure 4

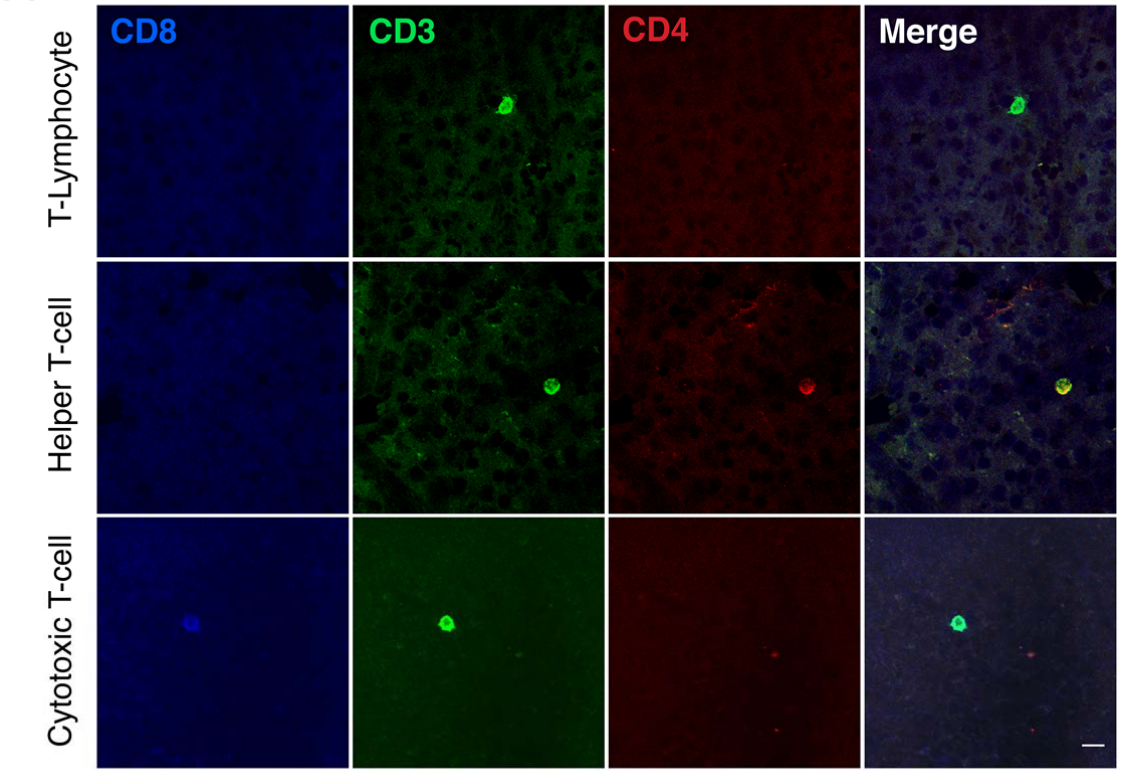

C *Cd3* - correlations

	Pearson rank		Pearson *r*	
Gene	Normal	Blast	Normal	Blast
Cxcr3	2510	3	0.684	0.898
Ccl4	668	406	0.746	0.814
Ifng	1823	443	0.704	0.812

Figure 4: (A) Micrographs of lymphocytes invading the retina. CD3 positivity identifies these cells as T-lymphocytes. Co-staining of CD3 and CD4 indicates Helper T-cells, and combined CD3/CD8 positivity identifies cytotoxic T-cells. Scale bar = 10µm. (B) Time course of lymphocyte counts in flat-mounted retinas. No lymphocytes were found in the control situation. There is an initial increase of CD3+ lymphocytes at 7 days after blast. As CD3+ cells decrease, the number of CD4+ and CD8+ cells increases over the course of a month. The grey shaded area denotes the 95%

confidence interval per group. (C) Correlations of *Cd3* to the cytokine-related genes *Cxcr3* (chemokine receptor 3), *Ccl4* (chemokine ligand 4) and *Ifng* (Interferon gamma). A drastic increase in ranked correlation and Pearson's correlation coefficient after blast can be seen.

Journal of Neurotrauma
Transcriptional Changes in the Mouse Retina Following Ocular Blast Injury: A Role for the Immune System (doi: 10.1089/neu.2017.5104)
This paper has been peer-reviewed and accepted for publication, but has yet to undergo copyediting and proof correction. The final published version may differ from this proof.

Figure 5

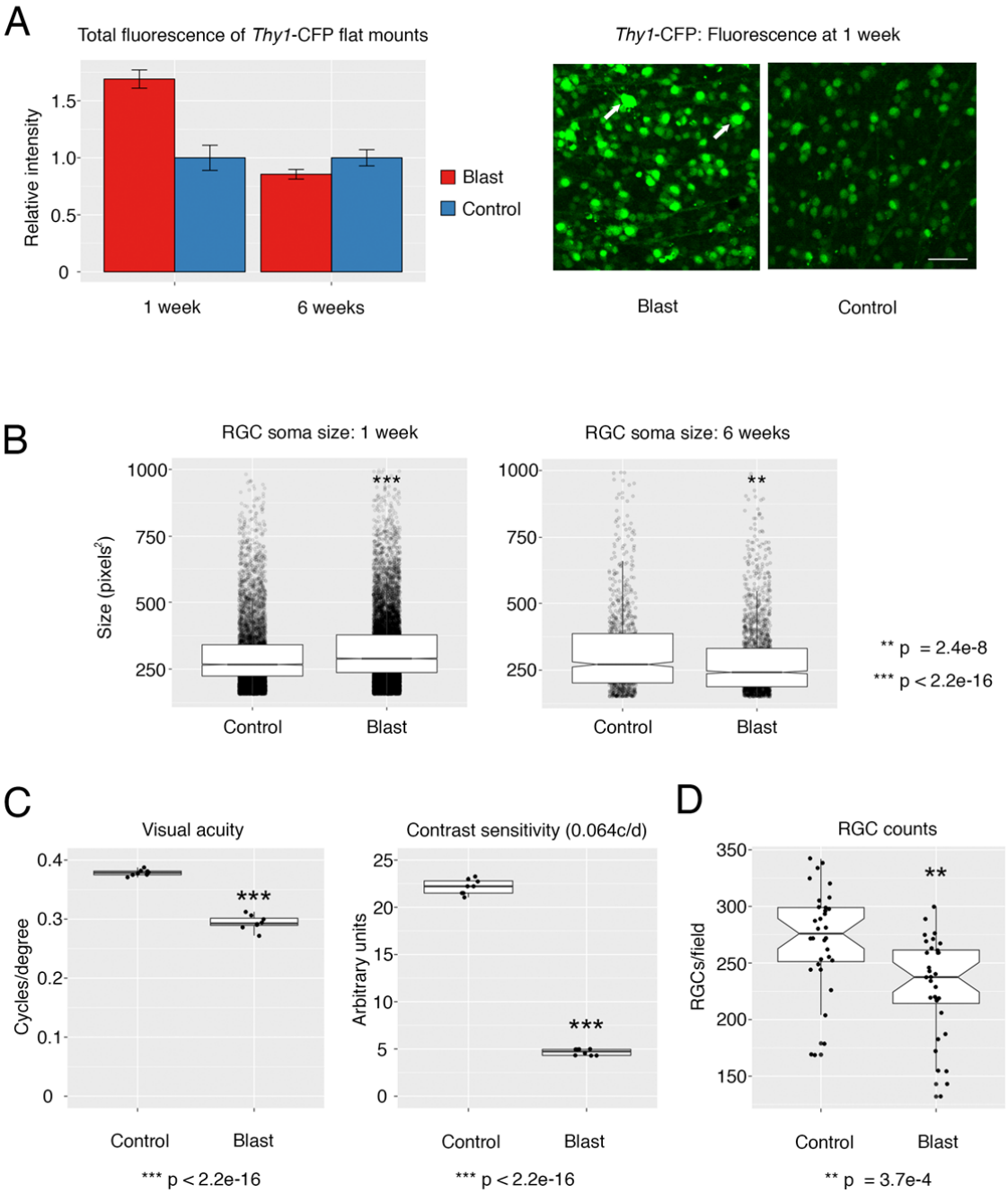

Figure 5: (A) Measurements of *Thy1*-CFP fluorescence in retinal flat mounts at 1 and 6 weeks after blast. The micrographs on the right are representative of the hyper-fluorescence seen 1 week after blast. Arrows indicate *Thy1*-CFP positive cells with very large somata. Scale bar = 100µm. Control vs Blast at 1 week, p<0.001, n=3 per condition. (B) Automated RGC soma size measurements at 1 and

6 weeks after blast. Soma size is significantly larger at 1 week after blast but significantly smaller at 6 weeks after blast. (C) Visual acuity and contrast sensitivity 6 weeks after blast. Both measures drop significantly after compared to a control situation. (D) RGC counts in retinal *Thy1*-CFP flat mounts. There is a significant drop 6 weeks after mice have been subjected to blast injury.

Journal of Neurotrauma
Transcriptional Changes in the Mouse Retina Following Ocular Blast Injury: A Role for the Immune System (doi: 10.1089/neu.2017.5104)
This paper has been peer-reviewed and accepted for publication, but has yet to undergo copyediting and proof correction. The final published version may differ from this proof.

Figure 6

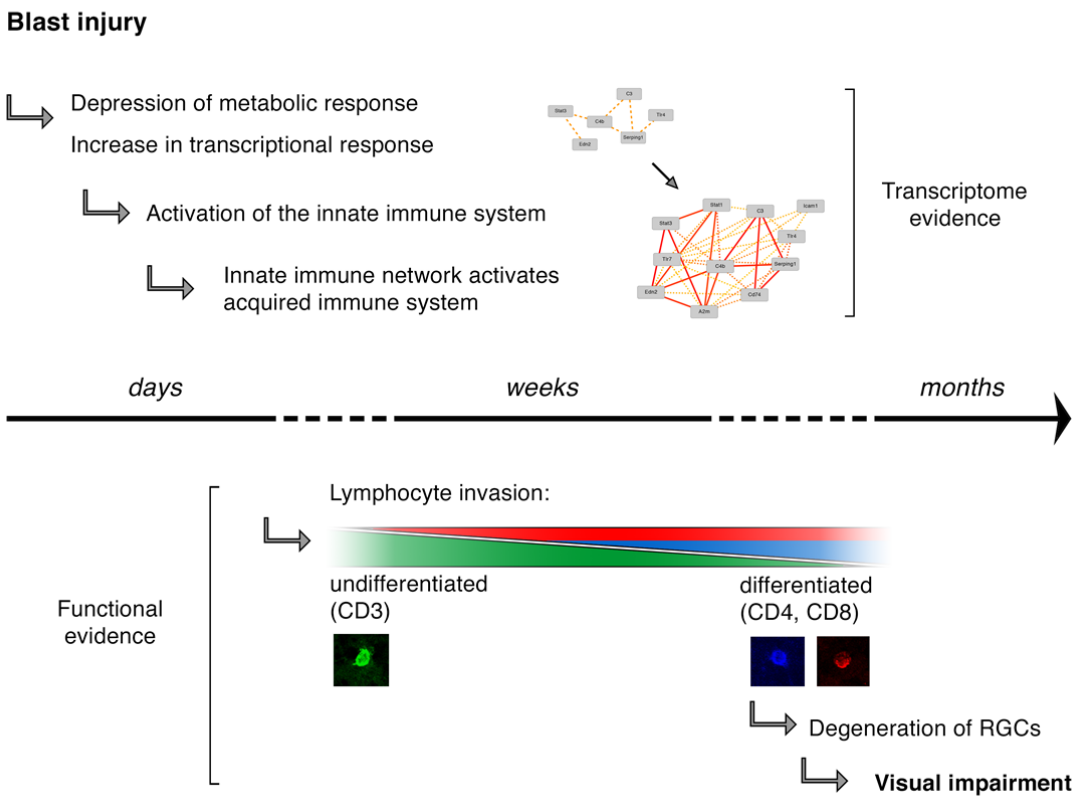

Figure 6: Diagram summarizing the main findings of this study. Over the course of days and weeks, the moderate transcriptional changes seen in the retina lead to activation of the innate and the acquired immune networks, which in turn results in chronic neurodegeneration and visual impairment months after injury.

Table 1: Genes associated with the innate immune system. There is a slight increase of RNA expression and strong increase in correlation. Correlation values and their associated p-value are in relation to *C4b*.

Journal of Neurotrauma
Transcriptional Changes in the Mouse Retina Following Ocular Blast Injury: A Role for the Immune System (DOI: 10.1089/neu.2017.5104)
This paper has been peer-reviewed and accepted for publication, but has yet to undergo copyediting and proof correction. The final published version may differ from this proof.

Supplementary Figure 1

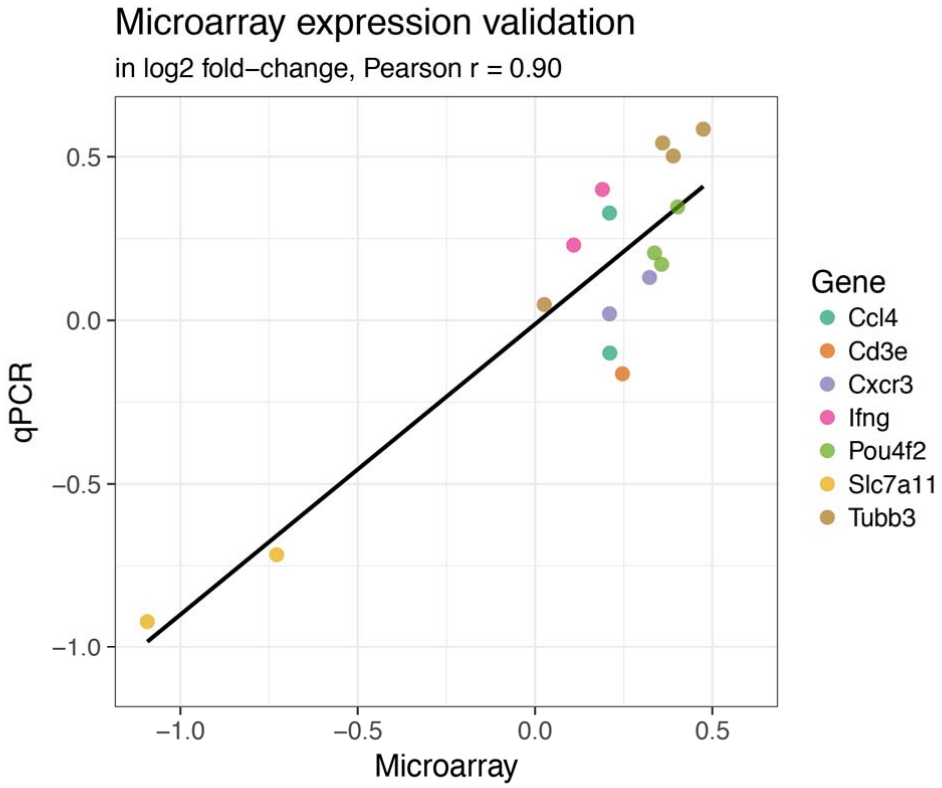

Gene	Strain	Microarray FC	qPCR FC
Cd3e	BXD27	0.246	−0.163
Tubb3	BXD27	0.026	0.048
Pou4f2	BXD42	0.337	0.206
Tubb3	BXD42	0.360	0.542
Slc7a11	BXD75	−1.093	−0.921
Pou4f2	BXD75	0.357	0.171
Tubb3	BXD75	0.390	0.502
Slc7a11	BXD85	−0.728	−0.716
Pou4f2	BXD85	0.402	0.347
Tubb3	BXD85	0.474	0.584
Cxcr3	B6	0.323	0.131
Ccl4	B6	0.210	0.328
Ifng	B6	0.190	0.400
Cxcr3	D2	0.210	0.020
Ccl4	D2	0.211	−0.100
Ifng	D2	0.109	0.230

Primers used (5' --> 3')

Slc7a11 fw	GGTGTGTAATGATAGGGCAGCA
Slc7a11 rev	CGGTCGTGACTTCCCCTTTG
Cd3e fw	TCTGGGCTTGCTGATGGTCAT
Cd3e rev	GTTCCTCGGGTCACAGGCTT
Ifng fw	TCAGCAACAGCAAGGCGAAA
Ifng rev	GCGACTCCTTTTCCGCTTCC
Pou4f2 fw	TGAACCCAGACCAAGCCAGG
Pou4f2 rev	GGTGCAGTTAAAGGGGACAGC
Tubb3 fw	CCTTTTCGTCTCTAGCCGCG
Tubb3 rev	CCTATCTGGTTGCCGCACTG
Ccl4 fw	CAAACCTAACCCCGAGCAACA
Ccl4 rev	GCAGGAAGTGGGAGGGTCAG
Cxcr3 fw	ACCAGCCAAGCCATGTACCTT
Cxcr3 rev	CGTAGGGAGAGGTGCTGTTTT

Supplementary Figure 1: Validation of microarray expression data and samples/primers used. qPCR-derived fold changes values were $\log_2$ transformed and plotted against microarray expression data. There is good agreement of qPCR and microarray data (Pearson's r = 0.90).

Journal of Neurotrauma
Transcriptional Changes in the Mouse Retina Following Ocular Blast Injury: A Role for the Immune System (DOI: 10.1089/neu.2017.5104)
This paper has been peer-reviewed and accepted for publication, but has yet to undergo copyediting and proof correction. The final published version may differ from this proof.

Journal of Neurotrauma
Transcriptional Changes in the Mouse Retina Following Ocular Blast Injury: A Role for the Immune System (DOI: 10.1089/neu.2017.5104)
This paper has been peer-reviewed and accepted for publication, but has yet to undergo copyediting and proof correction. The final published version may differ from this proof.

Supplementary Figure 2

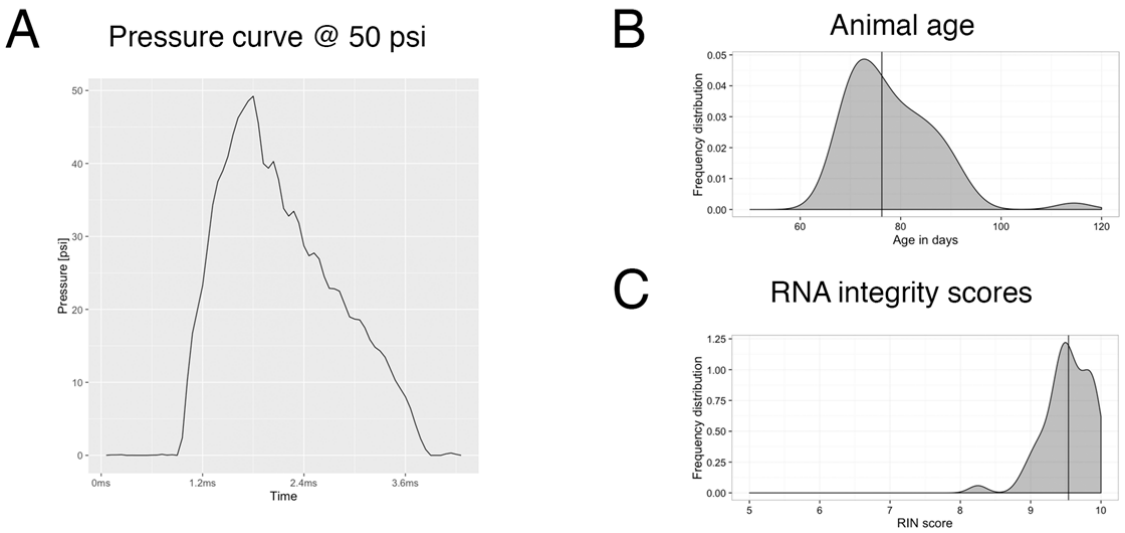

Supplementary Figure 2: (A) A typical pressure curve produced by the blast gun. (B) Distribution of animal age for blast samples. (C) Distribution of RIN scores for blast samples. The vertical line in (B) and (C) represents the median.

Journal of Neurotrauma
Transcriptional Changes in the Mouse Retina Following Ocular Blast Injury: A Role for the Immune System (DOI: 10.1089/neu.2017.5104)
This paper has been peer-reviewed and accepted for publication, but has yet to undergo copyediting and proof correction. The final published version may differ from this proof.

Supplementary Figure 3

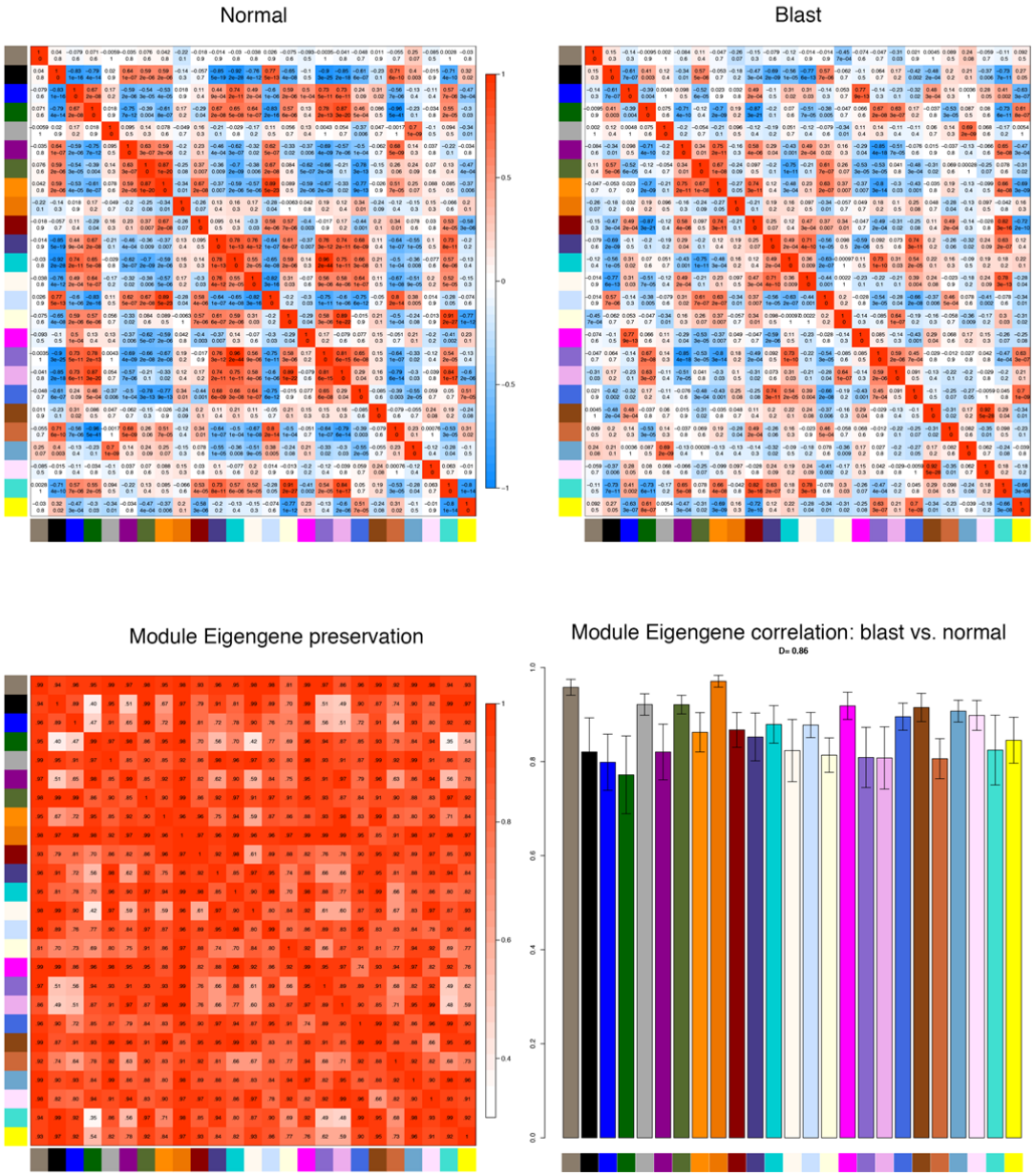

Supplementary Figure 3: Top: Correlation matrices of WGCNA modules identified for the blast and normal datasets. The colors on the x- and y-axis represent the module. Bottom left: Module eigengene preservation between both conditions. Lower values indicate higher intermodular changes. Bottom right: Module eigengene correlation between both condition. Lower values indicate stronger intramodular changes between conditions.